International Journal of Applied Pharmaceutics

ISSN- 0975-7058 Vol 17, Issue 1, 2025

Original Article

# CILNIDIPINE-LOADED TRANSDERMAL NANOEMULSION-BASED GEL: SYNTHESIS, OPTIMISATION, CHARACTERISATION, AND PHARMACOKINETIC EVALUATION

**MAHESH T. GAIKWAD[1*], RAJENDRA P. MARATHE[2]**

[1*]Govt College of Pharmacy, Opp. Govt. Polytechnic, Osmanpura, Chhatrapati Sambhajinagar-431005, Maharashtra, India. [2]Department of Pharmaceutical Chemistry, Govt College of Pharmacy, Opp. Govt. Polytechnic, Osmanpura, Chhatrapati Sambhajinagar-431005, Maharashtra, India

*Corresponding author: Raman Rajeshkumar; *Email: maheshgaik7@gmail.com

*Received: 16 Sep 2024, Revised and Accepted: 02 Nov 2024*

**ABSTRACT**

**Objective:** The aim of the study was to enhance transdermal flux and bioavailability, thereby reforming the effectiveness of drug delivery by synthesising and characterising cilnidipine-loaded nanoemulsion-based gel.

**Methods:** The research was conducted with meticulous planning and execution. After preformulation studies, cilnidipine-loaded nanoemulsions were synthesised using probe sonication and optimised by a 2-factor central composite design. The optimised nanoemulsions were loaded in Carbopol 940 and HPMC $K_4M$ gelling system. The optimised nanoemulsions were characterised for droplet size, zeta potential, viscosity, refractive index, pH and TEM, and cilnidipine-loaded nanoemulsion gels were characterised for clarity, homogeneity, consistency, spreadability, extrudability, pH, viscosity, *in vitro* diffusion study, dermal toxicity, and pharmacokinetic profiling. The process was accurately planned and accomplished at each step to ensure the precision and reliability of the results.

**Results**: The findings of this research are not just significant; they are groundbreaking. The steady-state flux values observed ranged from 35.71±1.27 µg/cm$^2$/h to 107.7±2.04 µg/cm$^2$/h for DOE_CiL_1 to 9 and 40.88±1.44 µg/cm$^2$/h to 80.64±1.38 µg/cm$^2$/h for NEn_CiL_GeL_1 to 4. These results underscore the diverse efficacy of different formulations in facilitating drug delivery through the skin. The pharmacokinetics profile of cilnidipine also showed remarkable changes. The $C_{max}$ for the cilnidipine tablet was 332.3±14.2 ng/ml, whereas it significantly increased ($p<0.05$) to 593.00±24.8 ng/ml in the nanoemulsion gel, demonstrating a substantial enhancement in drug concentration. Additionally, the $AUC_{0-12}$ showed a significant ($p<0.05$) increase from 1279±34.1 ng/ml. h with the tablet to 1922.50±162.8 ng/ml. h with the nanoemulsion gel. The $AUC_{0-\infty}$ also increased from 1395.5±156.7 ng/ml·h for the tablet to 1962.30±174.9 ng/ml. h for the nanoemulsion gel, further confirming the improved bioavailability of cilnidipine with the nanoemulsion gel. These significant bioavailability improvements cause excitement about the potential impact of this research, which could revolutionise transdermal drug delivery systems in the pharmaceutical business, leading to more effective and efficient drug delivery methods.

**Conclusion:** The results of this novel study are not only promising but also hold the potential to be transformative. The significant improvement in transdermal flux from the cilnidipine-loaded nanoemulsion gel reveals a substantial increase in the drug's bioavailability. This breakthrough could eliminate several drawbacks of cilnidipine, like first-pass fate and poor solubility, and provide a safer, more convenient delivery method for managing hypertension.

**Keywords**: Cilnidipine, Pseudo-ternary phase diagram, Transdermal flux, Bioavailability, Pharmacokinetics, Dermal toxicity


DOI: https://dx.doi.org/10.22159/ijap.2025v17i1.52689 Journal homepage: https://innovareacademics.in/journals/index.php/ijap

## INTRODUCTION

High blood pressure is a significant cause of cardiovascular disorders, renal failure, and death if not detected and treated appropriately, affecting more than nearly 213 million by the year 2025. In this context, Cilnidipine, a novel class of anti-hypertensive medication that is different from other L-type $Ca^{2+}$channel blockers or even other antihypertensives that work against both l and N types and is a recently identified calcium channel blocker, was chosen as the drug of interest for this research. Because N-type calcium is distributed throughout the nerve and brain, it is expected to affect nerve action. This data will aid in selecting antihypertensive medications [1, 2].

Cilnidipine (CiL) is a poorly water-soluble drug with a Biopharmaceutical Classification System (BCS) Class II. It has a slow dissolution rate, hence poor bioavailability (<13%) in humans, and reported a pKa value of 11.39. It is highly hydrophobic, and its partition coefficient value is 4.7; thus, it has good permeability [3–8]. Despite its poor oral efficacy, cilnidipine is considered safer and more effective than other calcium antagonists in the treatment of hypertension [3]. However, as indicated, its high solubility and prolonged first-pass metabolism led to a very low oral bioavailability [9]. Previous research showed various methods for improving solubility and bioavailability and eradicating the drawbacks of cilnidipine. Strategies like self-micro emulsifying drug delivery systems [10], transferosomes [11], polymeric nanoparticles [12], fast-dissolving tablets [13], nanosuspensions [14, 15], oral films [16], Microemulsions were tried [17]. Transdermal drug delivery may find benefit with patients suffering from long-lasting hypertensive situations. The stratum corneum restricts the drug's transport across the skin. Hence, many researchers reported nano vesicles like nanoemulsion, transferosomes, and some other nano or microcarriers for transdermal delivery of the drug [18]. Nanoemulsions are an excellent choice as a delivery system for transdermal drug delivery. They are a subcategory of emulsions with twenty to 500 nm globule sizes, sometimes called mini-emulsions. Nanoemulsions can deliver lipophilic drugs, which may show enhanced pharmacological action. Their robust stability extends their expiry, making them a unique and practical choice for drug delivery [19–21]. Non-magnetized views of stable nanoemulsions reveal them to be transparent or slightly transparent. Moreover, they do not cream or settle. They improve absorption and bioavailability and remove variability in absorption, it has been found [22]. Nanoemulsions are kinetically stable and are extensively used because of their low rheological properties and good optical characteristics [23]. Several theories have explained the benefits of nanoemulsions for transdermal drug delivery. A greater degree of drug solubilisation in the nanoemulsion system may amplify the thermodynamic activity directed toward the skin. Substances in nanoemulsions may improve drug absorption via the skin through enhanced permeation. Last, the drug's penetration rate from the nanoemulsion may be increased because it is easy to change a drug's affinity for the internal phase to favour partition

into the skin. These unique benefits make nanoemulsions a highly effective choice for transdermal drug delivery [24].

This research is at the forefront of innovation, aiming to design and synthesise a nanoemulsion and nanoemulsion gel for the transdermal delivery of cilnidipine. We are breaking new ground in drug delivery by enhancing solubility and transdermal flux. Transdermal delivery can avoid the first-pass effect, facilitating a more controlled and steady drug release into the bloodstream. This approach aims to maximize the therapeutic potential of cilnidipine by improving its systemic availability and seeking to reduce potential side effects.

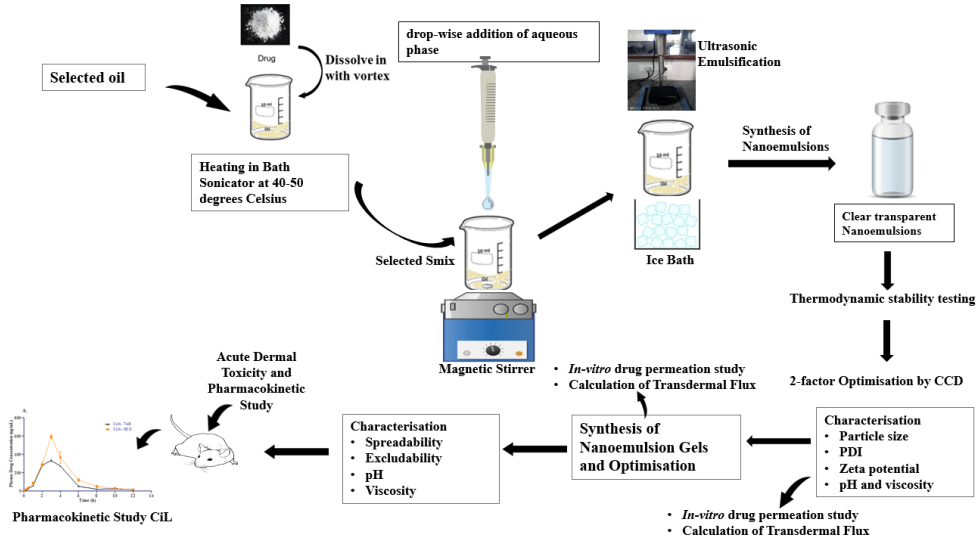


**Fig. 1: Graphical abstract showing synthesis and optimisation of cilnidipine nanoemulsions and cilnidipine-loaded nanoemulsion gel**

## MATERIALS AND METHODS

### Materials

Cilnidipine (CiL) was purchased from Yarrow Chem Products, Mumbai. IMCD India Private Ltd., Bandra (East), Mumbai provided gift samples of Polyoxyl 40 Hydrogenated Castor Oil (Kolliphor®RH40), Oleyl alcohol (Kollicream®OA), Macrogolglycerol Ricinoleate (Kolliphor®EL), and Macrogol (Kollisolv®PEG400). Glyceryl mono-oleate (Paceol), Oleoyl polyoxyl-6 glycerides (Labrafil®M 1944), Diethylene glycol monoethyl ether (Transcutol®P), Propylene glycol monolaurate (Lauroglycol™ FCC) were gifted by Gattefossé India, Vikhroli (East), Mumbai. Captex 355 was purchased from Abitee Corporation, USA. Glycerin, Triethanolamine, oleic acid, Ethanediol, Tween 20, Ethanol, Isopropyl alcohol, Isopropyl Myristate, PEG, PEG 200, and PEG 400 were procured from Thermo Fisher Scientific India Pvt. Ltd., Mumbai. Propylene glycol, Propanediol, and Ethyl oleate were procured from Loba Chemie Pvt Ltd., Mumbai. Hydroxy propyl methyl cellulose $K_4M$ and Carbopol 940 were obtained from Sigma-Aldrich Chemicals Pvt. Ltd, Bangalore. The solvents and remaining chemical compounds were all analytical grade. All of the excipients and chemicals were used precisely as obtained. A 0.45 µm membrane filter (Deccan Plastics, Pvt. Ltd., Chh. Sambhajinagar, India) was used to filter recently produced distilled water and when needed.

### Animals

Healthy Sprague Dawley and Wistar rats (Male and female) were procured from LACSMI Biofarms Pvt Ltd, Pune, and used. Before commencing the experiments, the Institutional Animal Ethical Committee (IAEC) approved the experimental animal studies (PCP/IAEC/2023/3-43 and PCP/IAEC/2023/3-44).

### Methods

### Preformulation assessment

### Solubility study of cilnidipine

The solubility of Cilnidipine was assessed using the shake flask system and measured in various oils, emulsifiers, and co-emulsifiers. As per the methodology, these solvents were mixed with the right amount of cilnidipine in 5 ml rubber-stoppered vials and 2 ml of ethyl alcohol. The combination was then incubated for 48 h at 37 °C in an orbital-shaker incubator (Remi Instruments, India). After ten minutes of centrifugation at 5000 rpm, the supernatants were filtered across a 0.45 µm membrane filter (Deccan Plastics, Pvt. Ltd., Chh. Sambhajinagar, India.) to remove any remaining particles. The solubility of cilnidipine was determined by back dilution and quantified using a UV spectrophotometer set at 243 nm. Each experiment was carried out thrice to ensure consistent and dependable results, reinforcing the reliability of our findings. Fig. 3 shows various components which solubilise the maximum amount of the drug chosen for the study [25, 26].

### Drug's chemical compatibility: excipients

100 mg of cilnidipine and 500 mg of each selected excipient were carefully weighed and combined into five-milliliter glass vials with rubber stoppers. Blends were maintained for 14 d in sealed vials in humidity-controlled ovens at 60 °C and 40 °C/75% RH. A pure standard cilnidipine sample was stored under the same conditions. Two sets of drug-excipient combinations were analysed using FTIR and DSC approaches after 14 d, as shown in fig. 4 [26–29].

### Surfactant and co-surfactant testing: evaluation of the emulsification efficiency

The emulsification properties were evaluated through visual inspection. A specified amount of oil and emulsifier were measured and blended in a 1:3 ratio to create a uniform mixture. The mixture was thoroughly heated at 40-50 °C to promise uniformity. Subsequently, 500 mg of the oil-surfactant mix was added to a 10 ml beaker and gradually blended with a magnetic mixture until dissolved. The degree of self-emulsification was optically assessed based on the last appearance, dispersibility, and comfort of emulsification, as indicated in table 1, and up to 10 ml of water was increasingly added. Different co-surfactants were evaluated by mixing specific emulsifiers in a 2:1 (w/w) mass ratio with co-surfactants. To ensure a homogenous blend, the oily component was added to the mixture at 1:3 (w/w), thoroughly vortexed, and heated softly. This practical line evaluated the co-surfactants' capability to emulsify [26].

**Table 1: Evaluation of the emulsification efficiency**

| Dispersibility and occurrence | Self-emulsification time (min) | Score | Reference |
|---|---|---|---|
| Make a clear, transparent nanoemulsion by rapidly dispersing in water | <1 | +++(very good) | [26] |
| The blend disperses into droplets that create a turbid emulsion in the water | 3–5 | +(good) | |
| The mixture forms clusters of oil droplets that stay together in the water | Not emulsified | -(Poor) | |

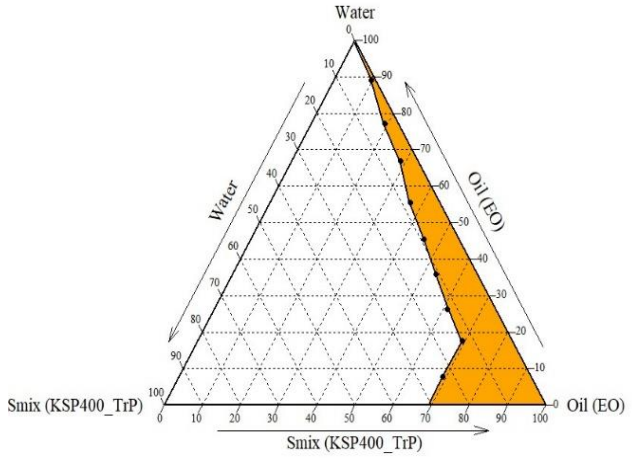


**A**

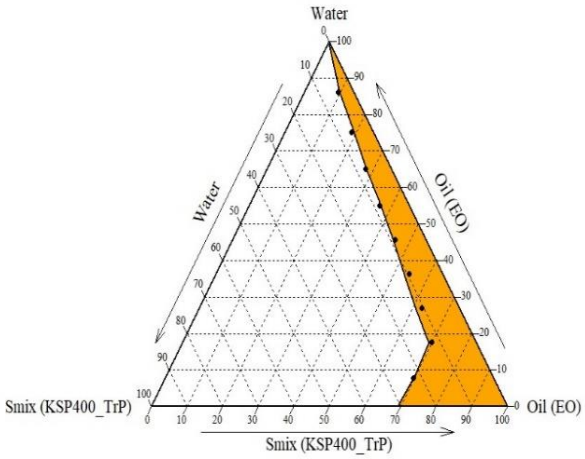


**B**

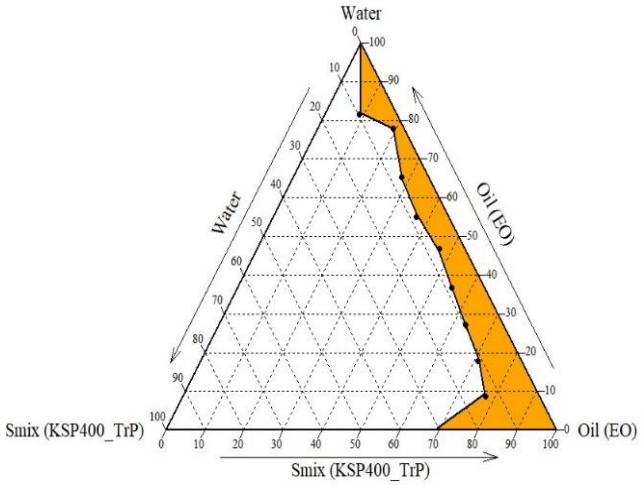


**C**

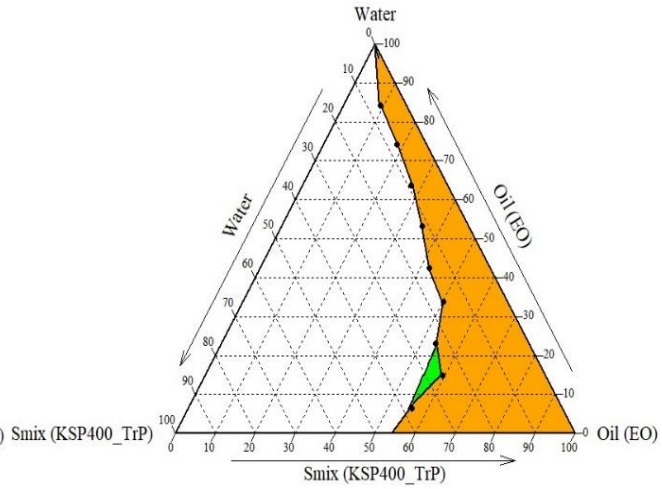


**D**

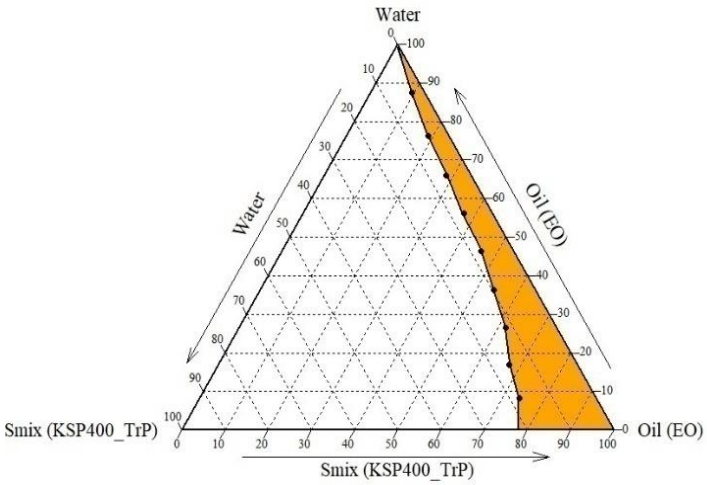


**E**

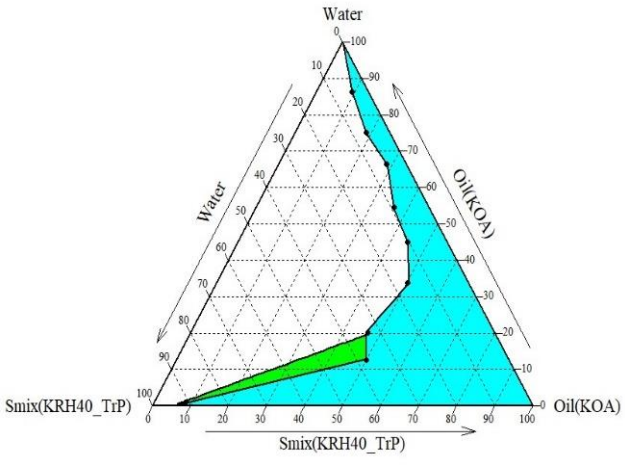


**F**

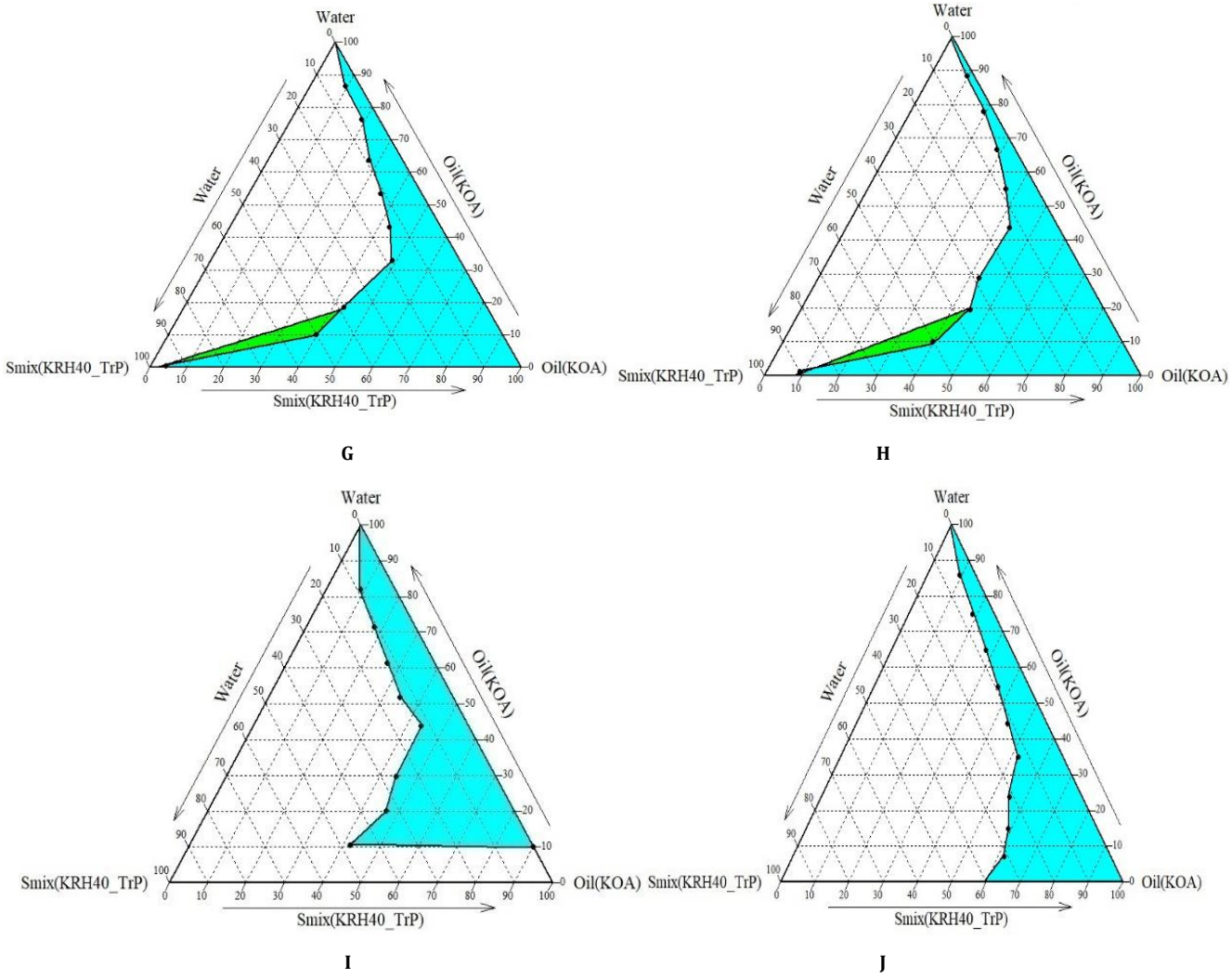


**Fig. 2: Pseudo-ternary phase diagrams, A) Ethyl Oleate with $S_{mix}$ (Kollisolve®PEG400: Transcutol®P) 1:1, B) Ethyl Oleate with $S_{mix}$ (Kollisolve®PEG400: Transcutol®P) 1:2, C) Ethyl Oleate with $S_{mix}$ (Kollisolve®PEG400: Transcutol®P) 1:3, D) Ethyl Oleate with $S_{mix}$ (Kollisolve®PEG400: Transcutol®P) 3:1, E) Ethyl Oleate with $S_{mix}$ (Kollisolve®PEG400: Transcutol®P) 3:2, F) Kollicream®OA with $S_{mix}$ (Kolliphor®RH40: Transcutol®P) 1:1, G) Kollicream®OA with $S_{mix}$ (Kolliphor®RH40: Transcutol®P) 1:2, H) Kollicream®OA with $S_{mix}$ (Kolliphor®RH40: Transcutol®P) 1:3, I) Kollicream®OA with $S_{mix}$ (Kolliphor®RH40: Transcutol®P) 3:1, J) Kollicream®OA with $S_{mix}$ (Kolliphor®RH40: Transcutol®P) 3:2**

**Synthesis and characterisation of cilnidipine nanoemulsion**

**Creation of pseudo-ternary phase diagrams**

Created pseudo-ternary phase diagrams are shown in fig. 2. This study used triple combinations with diverse oil ratios, emulsifiers, co-surfactants, and Chemix application ver. 10 was used to generate them. Kollisolve®PEG 400 and Kolliphor®RH40's self-emulsification ability played a role in the surfactant selection. The oil phase consisted of Kollicream®OA and ethylene oleate, with Transcutol®P as a co-surfactant. Less emulsification area led to the rejection of ethyl oleate. Pseudo-ternary phase diagrams were created using distilled water, $S_{mix}$, and oil. The water titration method was used to make it. The increasing surfactant concentration relative to co-surfactant and vice-versa resulted in the identification of different mass ratios between them (1:1, 1:2, 1:3, 3:1, and 3 is to 2). The oil was blended in a discrete 10 ml borosilicate glass beaker with a weight ratio of 1:9 to 9:1 using a specified mixing ratio. Phase borders in each phase diagram were precisely created using 45 diverse ratios of oil to $S_{mix}$ (9:1, 8:2, 7:3 up to 1:9). When the various o/w Nanoemulsions were clear or somewhat bluish, the titration was ended, and water was calculated. Translucency was experienced as the oil and $S_{mix}$ combinations were diluted in the water phase. We discarded the remaining nanoemulsions. The mass percent of water, oil, and $S_{mix}$ were recorded at these terminations because the sum was 100 %. Phase diagrams showing the physical state of nanoemulsions revealed the gathering of the $S_{mix}$ phase, oil phase, and aqueous phase in a single region. Each diagram described the nanoemulsion area, with a more extensive region indicating more efficient emulsification [30, 31].

**Formulation of cilnidipine-loaded nanoemulsions**

Cilnidipine is carefully added to the nanoemulsion system after investigating pseudo-ternary phase diagrams showing a more extensive nano-emulsification region. Kollicream®OA, surfactant-co-emulsifier mixture 1:3; (Kolliphor®RH40/Transcutol®P) were used. A weighed amount of cilnidipine is added to the oil in a 10 ml beaker, heated at 40 to 50 °C in a bath sonicator (Enertech Pvt. Ltd., Mumbai, India) with vortexing it, and then slowly mixed with calculated $S_{mix}$. The resultant mixture was titrated against water, and this assembly was placed over a magnetic stirrer (1 MLH Magnetic Stirrer, Remi Instruments, Mumbai, India) at 500 rpm to produce a raw emulsion. Droplet size was reduced using probe sonication from 0.33 min to<6 min, giving fine nanoemulsions [32–34].

**Table 2: Trial batches of cilnidipine nanoemulsions with ethyl oleate**

| $S_{mix}$ ratio | Formulation code | % w/w components in formulation | | |
|---|---|---|---|---|
| | | Oil (%) | Water (%) | $S_{mix}$ (S+CoS %) |
| NEn-A | NEn_CiL_A1 | 7.5 | 36 | 56.5 |
| $S_{mix}$ ratio 3:1 | NEn_CiL_A2 | 12.5 | 30 | 57.5 |
| | NEn_CiL_A3 | 17.5 | 26.7 | 55.8 |
| | NEn_CiL_A4 | 22.5 | 24 | 53.5 |

**Table 3: Trial batches of cilnidipine nanoemulsions with kollicream®OA**

| $S_{mix}$ ratio | Formulation code | % w/w components in formulation | | |
|---|---|---|---|---|
| | | Oil (%) | Water (%) | $S_{mix}$ (S+CoS %) |
| NEn-B | NEn_CiL_B1 | 5.2 | 75.2 | 19.6 |
| $S_{mix}$ ratio 1:1 | NEn_CiL_B2 | 10.2 | 58.7 | 31.1 |
| | NEn_CiL_B3 | 15.2 | 40.7 | 44.1 |
| | NEn_CiL_B4 | 20.2 | 33.2 | 46.6 |
| NEn-C | NEn_CiL_C1 | 3 | 83.6 | 13.4 |
| $S_{mix}$ ratio 1:3 | NEn_CiL_C2 | 8 | 63 | 29 |
| | NEn_CiL_C3 | 13 | 51.1 | 35.9 |
| | NEn_CiL_C4 | 18 | 40.6 | 41.4 |
| NEn-D | NEn_CiL_D1 | 5.2 | 77.8 | 17 |
| $S_{mix}$ ratio 1: 2 | NEn_CiL_D2 | 10.2 | 60.5 | 29.3 |
| | NEn_CiL_D3 | 15.2 | 45 | 39.8 |

**Optimisation of cilnidipine-loaded nanoemulsion by 2-factor central composite design**

Utilising response surface methodology (RSM), the analysis of independent variables was conducted, like a mixture of surfactant and co-surfactant [$S_{mix}$] (X1) and ultrasonic irradiation time (X2), affected response variables, such as drug content (Y2), particle size (Y1), and PDI (Y3) in nanoemulsions. In table 4, the central composite design and coded levels are displayed. A quadratic model and a central composite design (five levels) were used in the experiment's design. Table 9 lists the thirteen experimental runs, coded as Design of Experiment (DOE_CiL_1 to 9), and included five centre points (repeated, so only one is measured), four axial points, and four factorial points, so a total of nine runs were conducted randomly. Design-Expert®Software (Stat-Ease Inc., Trial version 13, Minnesa, USA) was employed in designing the experiment to create optimised cilnidipine-loaded nanoemulsions. Trail batch NEn_CiL_$C_2$ that underwent this optimisation [35–37].

**Table 4: Variables used in 2-factor central composite design**

| Independent variables | Levels | | | | |
|---|---|---|---|---|---|
| | -α | -1 | 0 | +1 | +α |
| X1: $S_{mix}$ (%) | 22.92 | 25 | 30 | 35 | 37.07 |
| X2: Ultrasonic irradiation time (min) | 0.1715 | 1 | 3 | 5 | 5.8284 |
| Dependent variables | | | | | |
| Y1: Particle size (nm) | Minimise | | | | |
| Y2: Drug content (%) | Maximise | | | | |
| Y3: PDI | Minimise | | | | |

**Thermodynamic stability studies**

Multiple thermodynamic stability tests were carried out to assess the physical stability of the formulations [38].

**Cycle of heating-cooling**

To evaluate the stability of the formulations, they were kept at 4° C in the refrigerator and 45° C for a minimum of 48 h, changing the temperature six times in succession [38].

**Test for centrifugation**

An investigation into phase separation and drug settling was conducted by centrifuging nanoemulsions for 30 min at 3000 rpm [38].

**Freeze-thaw cycle**

Three freeze-thaw series were employed throughout 48 h from temperatures-21 °C to 25 °C. [38].

**Characterisation of cilnidipine nanoemulsion**

**Cilnidipine nanoemulsion globule size measurement**

We used the Malvern particle size analyser (Zetasizer ver. 6.20, Model: MAL1051945, Malvern Instruments, Ltd., UK). The globule size of the nanoemulsions was assessed, with each size value stated as the mean±SD of three samples. The polydispersity index was computed to evaluate the uniformity of particle diameters [35, 38].

**Zeta Potential estimation of cilnidipine nanoemulsion globules**

Electrophoretic light scattering with a Malvern Zetasizer (Zetasizer ver. 6.20, Model: MAL1051945, Malvern Instruments, Ltd., UK) was used to estimate the zeta potential of the cilnidipine nanoemulsion. The experiment was conducted with a constant electrical field of 1 volt using a dynamic light scattering particle size analyser set to 633 nm. The nanoemulsion was diluted at a 1:100 ratio using pre-filtered, double-distilled water. The information was presented as mean±SD based on three separate assessments [35, 38].

**Viscosity**

A Brookfield RST rheometer (Brookfield Engineering Laboratories, Mumbai) with a MS: CCT-14 was used to measure the viscosity of the cilnidipine nanoemulsions at 25 °C. Three measurements were made [35, 38].

**Refractive index**

The nanoemulsion's refractive index was determined by applying one drop in triplicate to the slide at 25 °C using a refractometer (Cyber-Lab, Cyber AB, Hyderabad) [35, 38].

**pH determination**

The apparent pH of the cilnidipine nanoemulsion was determined using a pH meter in triplicate at 25 °C (Systronics, model 802, India) [35, 38].

**Transmission electron microscopy (TEM)**

The morphology of the cilnidipine nanoemulsion was examined. To ascertain its dimensions and form, a point-to-point-separable Gatan 626 cryo specimen holder electron microscope (TECNAI 12, Fei Company, The Netherlands, Software: Tecnai Imaging and Analysis, Source: Tungsten Filament) operating at 20–120 kV was utilised. Bright-field imaging techniques and diffraction modes were applied [35, 38].

***In vitro* permeation study for optimised cilnidipine-loaded nanoemulsions**

*In vitro* skin permeation experiments were carried out using Franz diffusion cells. To simulate the skin, the donor and receptor compartments were separated by the Dialysis Membrane-60, with a molecular size of 12000 Da. (Hi-Media Laboratories Pvt. Limited, Thane). Additionally, the dialysis membrane received the calculated dosage of optimised nanoemulsion, equivalent to 10 mg of medication. A 3 x 12 mm magnetic bead (Orchid Scientific and Innovative India Pvt. Ltd., Nashik, India) was utilised to ensure the drug was distributed uniformly and at the proper temperature. The medium used in this experiment consisted of 75% phosphate buffer 7.4 and 25% isopropyl alcohol. Approximately 1 ml of samples was taken from the receptor compartment at 0.5, 1, 2, 4, 6, 8, 12, and 24 h. These samples were then replaced with equivalent medium volumes to maintain sink condition. The dialysis membrane's total drug penetration was measured at μg/cm². The steady-state flux (μg/cm²/h) was the slope of the steady part of the graph, and the permeability coefficient was determined by dividing flux by concentration in the donor compartment, as indicated in fig. 16, table 15 [35, 39].

**Formulation and optimisation of cilnidipine-loaded nanoemulsion-gel**

For this investigation, first, we prepared 20 different simple gel formulations [(Coded as SG1-SG20)-Data Hidden] using HPMC $K_4M$ and Carbopol 940 as gelling agents, with their percentages ranging from 0.25 to 1.5 % with an increment of 0.25 %. Glycerin was used 5-10 % for ten simple gel formulations with HPMC $K_4M$ and ten with Carbopol 940. A methodologically weighed amount of Carbopol 940 was added to 100 ml of distilled water to swell overnight. HPMC $K_4M$ was separately dispersed in hot water at a slightly modified temperature at 80 °C and stirred till room temperature. Other excipients were slowly added with continuous stirring, and a sonicator was used for 10 min to remove the trapped air. Finally, triethanolamine was added to adjust pH 6 to 6.8. These simple gels were optimised by checking viscosity and spreadability, and only eight formulations (HPMC $K_4M$ and Carbopol 940 with 1 and 1.5 %) were selected for further study, as reported in table 5 [40–43]. SG 19 was selected based on its characterisation for the nanoemulsion gelling process. 40 g of Optimised nanoemulsion DOE_CIL_7 was slowly and continuously stirred with 14 g of simple gel SG 19 to get approximately 54 g of cilnidipine-loaded nanoemulsion gel, as shown in table 6 [40, 41, 44].

**Table 5: Simple gel (SG) formulations**

| Formulation code | HPMC K4M % w/w | Carbopol 940 % w/w | PEG 400 % w/w | Glycerol % w/w | Methylparaben | Peppermint oil | Triethanolamine w/w | Distilled water |
|---|---|---|---|---|---|---|---|---|
| SG4 | 1 | | 5 | 5 | 0.03 | 0.2 | Q. S. | Q. S 100 |
| SG5 | 1.5 | | 5 | 5 | 0.03 | 0.2 | Q. S. | Q. S 100 |
| SG9 | 1 | | 5 | 10 | 0.03 | 0.2 | Q. S. | Q. S 100 |
| SG10 | 1.5 | | 5 | 10 | 0.03 | 0.2 | Q. S. | Q. S 100 |
| SG14 | | 1 | 5 | 5 | 0.03 | 0.2 | Q. S. | Q. S 100 |
| SG15 | | 1.5 | 5 | 5 | 0.03 | 0.2 | Q. S. | Q. S 100 |
| SG19 | | 1 | 5 | 10 | 0.03 | 0.2 | Q. S. | Q. S 100 |
| SG20 | | 1.5 | 5 | 10 | 0.03 | 0.2 | Q. S. | Q. S 100 |

**Table 6: Cilnidipine-loaded nanoemulsion gels**

| Ingredients | | | | | | Cilnidipine-loaded optimized nanoemulsion | | | |
|---|---|---|---|---|---|---|---|---|---|
| Formulation code | Cilnidipine % | Carbopol 940 gel 1 % | Carbopol 940 Gel 1.5 % | HPMC K4M gel 1 % | HPMC K4M gel 1.5 % | Mls of nanoemulsion added | KOA | Smix | Water |
| NEn_CiL_1 | 0.201 | 14 gm | | | | 40 | 8 | 30 | 62 |
| NEn_CiL_2 | 0.201 | | 14 gm | | | 40 | 8 | 30 | 62 |
| NEn_CiL_3 | 0.201 | | | 14 gm | | 40 | 8 | 30 | 62 |
| NEn_CiL_4 | 0.201 | | | | 14 gm | 40 | 8 | 30 | 62 |

**Characterization of cilnidipine-loaded nanoemulsion-gel**

**Exterior appearance, pH, and viscosity**

The prepared gel's exterior appearance, pH, and viscosity were examined. Visual evaluation was done to determine the nanoemulsion gel's clarity, consistency, and homogeneity. The pH of the optimised gel was measured using a digital pH meter (Model 802, Systronics, India) at room temperature using a 1 percent solution of nanoemulsion gel. A Brookfield RST rheometer (Brookfield Engineering Laboratories, Mumbai) determined the viscosity of cilnidipine-loaded nanoemulsion gel at 25±3 °C. Three readings were taken [18, 35].

**Spreadability**

A lower glass slide turned into a constant in this block. An extra prepared nanoemulsion gel (approximately 1 gm) underneath the study was placed on this ground slide. The nanoemulsion gel formulation was then inserted among this slide and some other glass slides, which had the dimension of a fixed ground slide and turned into provided with a hook. To release air and create a consistent gel layer between the slides, a 100 g weight is placed on each slide for five minutes. Excess of the nanoemulsion gel was removed from the borers. The upper slide was then exposed to a tug of 25 g weight with the help of a cord linked to the hanger, and the time (in sec) required via the top slide to cover a distance of 7 cm was mentioned. A briefer interval indicates higher spreadability [41].

**Extrudability**

The capped collapsible aluminium tubes were filled with nanoemulsion gel formulations and sealed by crimping. We recorded the tube weights. Clamps were used to position the tubes between two glass slides. Afterwards, the cap was removed, and 50 g was placed over the slides. We counted and weighed the amount of extruded nanoemulsion gel [41].

### *In vitro* permeation study for cilnidipine-loaded nanoemulsion-based gel

*In vitro* skin permeation experiments were carried out using Franz diffusion cells. The dialysis membrane-60 separated the donor and receptor compartments to simulate the skin. The Donar compartment received 1.5 g of optimised nanoemulsion gel, equivalent to 0.2 % of the drug. The diffusion medium (75% phosphate buffer 7.4 and 25% isopropyl alcohol) was agitated using a Teflon-coated magnetic bead to maintain a constant drug circulation at 37±2 °C. About 1 ml of sample was taken from the receptor compartment at 0.5, 1, 2, 4, 6, 8, 12, and 24 h. These samples were replaced with equivalent medium volumes of diffusion media to maintain sink conditions. The dialysis membrane's total drug penetration was measured in µg/cm$^2$. Steady-state flux (µg/cm$^2$/h) is the slope of the linear part of the line, and the permeability coefficient is calculated by dividing the steady-state flux by the drug's concentration in the donor compartment, as indicated in fig. 17, table 16 [35, 39].

### Acute dermal toxicity study of cilnidipine-loaded nanoemulsion-based gel

In a study on acute dermal toxicity in female Wistar albino rats, the procedures were conducted per OECD Guideline No. 402. Fifteen healthy Wistar Albino rats weighing 200-250 g were divided into three groups. The standard control and test groups were prepared, each consisting of 5. Before the study commenced, the rats' backs were clipped and individually caged for 24 h. On the test day, the group received an optimised nanoemulsion gel of cilnidipine, which was evenly applied to the exposed skin. Over the next 14 d, the rats were observed twice daily for signs of irritation, changes in behavior, and mortality. Water intake, diet intake, and body mass were measured every day. The rats were sacrificed to examine and weigh their organs on the fifteenth day. This study focused on rat skin reactions, general health, and organ function to assess the acute dermal toxicity of cilnidipine-loaded nanoemulsion gels. Every animal in the study was observed daily to evaluate clinical indicators such as irritability, behavioural changes, toxicity symptoms, morbidity, and mortality. They were monitored closely for any changes or reactions, and detailed daily records of their clinical status were kept. Physiological parameters, including body weight, food and water consumption, and haematological and serum biochemical profiles, were assessed to fully comprehend the effect of the test substances on the animals' health [45–49].

### Pharmacokinetic study

15 Sprague Dawley rats were divided into five groups of 3 animals each. Standard Control/Control group (G1) animals have received no treatment. Animals of Group G2 and G3 were administrated orally with Marketed formulations of cilnidipine tablets at the doses of 1.1 mg/kg. The doses were calculated according to the reported method. Further, the skin on the abdominal side of groups G4 and G5 rats was shaved with depilated cream. For the test formulations, a cilnidipine-loaded nanoemulsion gel was applied topically. The rats underwent isoflurane anesthesia, and 500 µl** of blood was extracted from their retro-orbital plexus in EDTA tubes at various time breaks, including 0.25, 0.5, 1, 2, 3, 6, and 12 h. The blood samples were centrifuged at 3500-4000 rpm for 10-12 min. After separation, the blood plasma was kept at-21 °C. Then, drug analysis was carried out using a developed HPLC method [45–47, 49].

## RESULTS AND DISCUSSION

### Solubility study of cilnidipine

Based on the solubility of cilnidipine in various components, oils, surfactants, and cosurfactants were selected. Results revealed that cilnidipine has maximum solubility in oils Kollicream®OA38.2±2.36 and Ethyl Oleate 12.5±1.02. Maximum solubility found in surfactants Kolliphor®RH40 51.72±2.36, Kollisolv®PEG400 19.45±2.31 and co-surfactants like Ethanol 29.76±1.56 and in Transcutol®P 48.92±2.74. All other excipients with more solubility were rejected due to their less emulsification efficacy tested as per the protocol shown in table 1. All values represented in mg/ml are denoted in fig. 3.

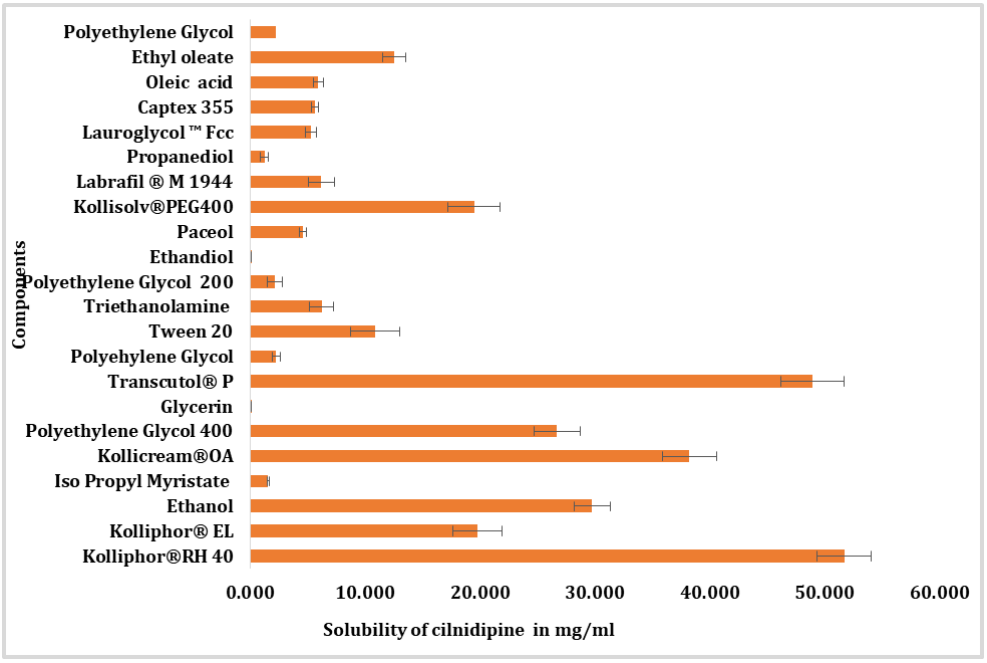


**Fig. 3: Solubility of cilnidipine in oils, surfactants, and co-surfactants, data represented as mean±SEM, n = 3 observations**

### Drug's chemical compatibility: excipients

Cilnidipine's FTIR spectroscopy and formulations with different excipients were essential to the formulation process. This study confirmed the integrity of critical functional groups and offered insightful information about molecular interactions. The particular absorption peaks showed no interaction with Kollicream®OA. Still, mild interactions with Koliphor®RH40, Transcutol®P, Kollisolv®PEG400, and ethyl oleate were shown, as illustrated in fig. 4. The analysis verified cilnidipine's molecular structure and purity, guaranteeing the creation of stable nanoemulsions.

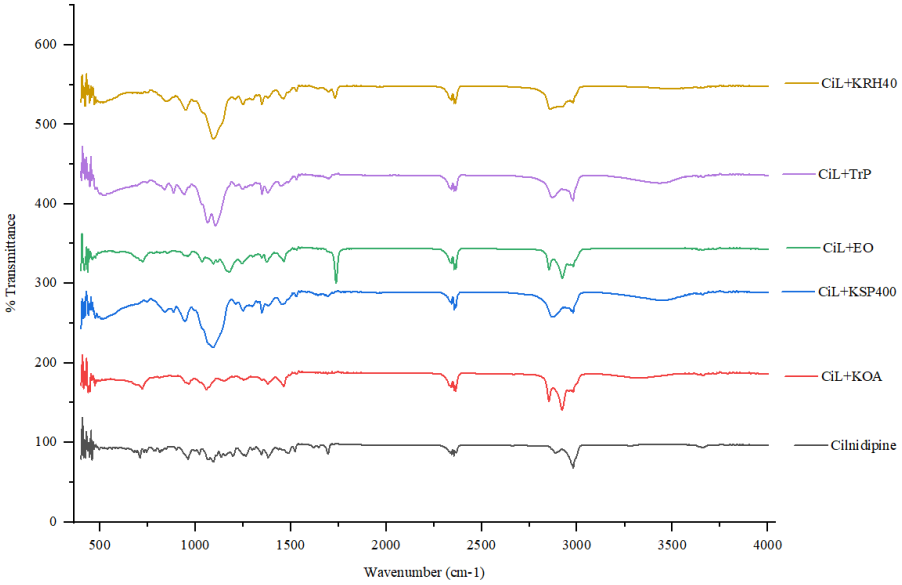


**Fig. 4: FTIR study of various components in 1:5 physical mixtures**

**Surfactant and co-surfactant testing: evaluation of the emulsification efficiency**

Emulsification efficacies research was carried out on components selected based on the solubility of oils, surfactants, and co-surfactants. A visual appraisal system is employed. Results showed that amongst Kollicream®OA, Ethyl Oleate and Paceol were selected as oil phases and tested against a series of surfactants, Kolliphor®RH40, Kolliphor®EL, Kollisolve®PEG 400 showed that Kolliphor®RH40 can emulsify Kollicream® OA, whereas Kollisolve® PEG 400 can emulsify Ethyl Oleate in 1:3 w/w mass ratios. Paceol was not emulsified. Selected surfactants were then studied against Ethanol and Transcutol®P as co-surfactants efficiency against oil. Hence, only Transcutol®P was able to emulsify oil in combination with 1% w/w oil. Results were demonstrated in table 7 and table 8.

**Table 7: Emulsification efficacy of emulsifier with selected oil (oil 1: surfactant 3) w/w**

| Emulsifier (3% w/w) | Oils (1% w/w) | | | | | |
|---|---|---|---|---|---|---|
| | Kollicream®OA | | | Ethyl Oleate | | |
| | Dispersibility and presence | Self-emulsification period (min) | Score | Dispersibility and presence | Self-emulsification period (min) | Score |
| Kolliphor®RH40 | The transparent spontaneous blue emulsion formed | 1-2 min | +++Very good | Turbid | >2 min | -Poor |
| Kollisolve®PEG400 | Turbid emulsion | >4 min | +Good | The clear spontaneous blue emulsion formed | 1-2 min | +++Very good |
| Kolliphor® EL | Turbid | >3 min | -Poor | Turbid | >4 min | -Poor |

**Table 8: Emulsification efficiencies of $S_{mix}$ combinations with oil (oil 1: surfactant 2:co-surfactant 1) w/w**

| Co-surfactant (1% w/w) | Oily phases (1% w/w) Kollicream®OA | | | | | |
|---|---|---|---|---|---|---|
| | Surfactant (2% w/w) | | | | | |
| | Kolliphor®RH40 | | | Kollisolve®PEG400 | | |
| | Dispersibility and presence | Self-emulsification period (min) | Score | Dispersibility and presence | Self-emulsification period (min) | Score |
| Transcutol®P | Clear nanoemulsion formed | <1 min | ++++Very good | Turbid | >2 min | -Poor |
| Ethanol | Turbid | >3 min | -Poor | Turbid | >3 min | -Poor |

**$S_{mix}$ mass ratio's impact on nanoemulsion region of pseudo-ternary phase diagram**

A pseudo-ternary phase diagram identifies the nanoemulsion region. Kollicream®OA and ethyl oleate were utilised as the oil phase. In the screening process, Transcutol®P was used as a co-surfactant, and Kolliphor®RH40 and Kollisolve®PEG400 were used as surfactants. Phase diagram investigation discovered that, as shown in fig. 2F to J, the primary region for nanoemulsions was identified in $S_{mix}$ proportions of 1:1 and 1:2. The maximum amounts of oil that could be soluble can be seen in these diagrams. Fig. 2F reveals a 30% wt/wt solubility at a 52.2 % wt/wt $S_{mix}$ ratio for 1:1 and 28% wt/wt solubility of Kollicream ®OA at a 55.5 % wt/wt $S_{mix}$ ratio for 1:2. Greater emulsification efficiency inside the system is shown by an increased nanoemulsion area fig. 2, Tables 7 and 8 show that Transcutol®P performed better than the other groups, probably because of its high cilnidipine solubility. Increasing the surfactant concentration at a 1:3 $S_{mix}$ ratio (fig. 2H) resulted in less region, and a 3:1, 3:2 $S_{mix}$ ratio (fig.2I, J) resulted in no nanoemulsion area. Therefore, experimenting with a 4:1 $S_{mix}$ ratio was pointless.

A decrease in the nanoemulsion region was noted after the surfactant concentration of $S_{mix}$ was raised from 1:1 to 3:1 for Kollicream ®OA. A low concentration of co-surfactant could explain

this, as it would lessen interfacial tension and increase the flexibility of the nanoemulsion region and interface. No nanoemulsion zone was found in fig. 2 A–D or fig. 2E for Ethyl Oleate, with a smaller nanoemulsion region [50, 51]. Our examination of the nanoemulsion area has produced significant recommendations for the effectiveness of drug delivery. The region shortened as the co-surfactant concentration rose from $S_{mix}$ 1:1 to $S_{mix}$ 3:2. As the co-surfactant concentration increased, the area shrank increasingly, reaching 3:1 and 3:2 $S_{mix}$ ratios. Phase diagrams optically illustrate how $S_{mix}$ declines interfacial tension and increases interfacial area. Introducing $S_{mix}$ can significantly lower the free energy of the nanoemulsion system to a minimum concentration, ensuring thermodynamic stability and presenting a hopeful method.

**Formulation of cilnidipine-loaded nanoemulsions**

NEn_CiL_A1 to A4 were synthesised from $S_{mix}$ mass ratio 3: 1, whereas $S_{mix}$ ratios 1:1, 1:2, one is to 3 were used to synthesise NEn_CiL_B1 to B4, C1 to C4, and D1 to D3. D4 is not synthesised due to gelling before water titration. NEn_CiL_C2 is selected for further optimisation as it contains less $S_{mix}$ concentration than others, which will justify the toxicity issues of $S_{mix}$. Not only was this phase separation observed in NEn_CiL_A1 and A2 after the Cycle of Heating-Cooling, but NEn_CiL_A3 and A4 were unstable after the Freeze-Thaw Cycle. NEn_CiL_B2, B3 shows increased viscosity, turbidity, and phase separation after the heating and cooling cycle. NEn_CiL_B4 shows a complete milky appearance. NEn_CiL_C1 and C3 have slight turbidity. C4 is slightly apparent, whereas NEn_CiL_B1 and C2 formed clear and stable nanoemulsions even after thermodynamic stability studies. Hence, NEn_CiL_C2 is selected for further optimization, as indicated in fig. 5.

**Optimisation of cilnidipine nanoemulsion**

**Investigation of optimization by 2-factor central composite design**

A comprehensive literature review was meticulously conducted before the synthesis of cilnidipine nanoemulsions. This step was crucial as it provided a solid foundation for selecting oils, a combination of emulsifiers and co-emulsifiers, based on proper emulsification analysis and the solubility of cilnidipine in each excipient. Subsequently, trial nanoemulsions were synthesised based on the nanoemulsion area in pseudo-ternary phase diagrams. The NEn_CiL_C2 batch was then chosen for optimisation.


**Fig. 5: Cilnidipine-loaded nanoemulsions (Trial batches)**

**Table 9: Optimisation by the central composite design of batch NEn_CiL_C2**

| | | Independent variables | | Dependent variables | | |
|---|---|---|---|---|---|---|
| **Batch code** | **Run** | **$S_{mix}$ (KOLRH40_TrP) factor 1** | **Ultrasonic irradiation time (min) factor 2** | **Particle size (nm) response 1** | **Drug content (%) response 2** | **PDI response 3** |
| DOE_CiL_1 | 1 | 30 | 0.1715 | 151.9 | 99.5 | 0.341 |
| DOE_CiL_2 | 2 | 35 | 5 | 215.2 | 100.1 | 0.321 |
| DOE_CiL_3 | 3 | 37.07 | 3 | 350 | 101 | 0.485 |
| DOE_CiL_4 | 4 | 25 | 5 | 105 | 99.2 | 0.125 |
| DOE_CiL_5 | 5 | 22.92 | 3 | 120 | 98.3 | 0.179 |
| DOE_CiL_6 | 6 | 30 | 5.8284 | 123.3 | 97.2 | 0.286 |
| DOE_CiL_7 | 7 | 30 | 3 | 97.70 | 99.8 | 0.384 |
| DOE_CiL_8 | 8 | 35 | 1 | 380 | 120 | 0.395 |
| DOE_CiL_9 | 9 | 25 | 1 | 120 | 101 | 0.215 |

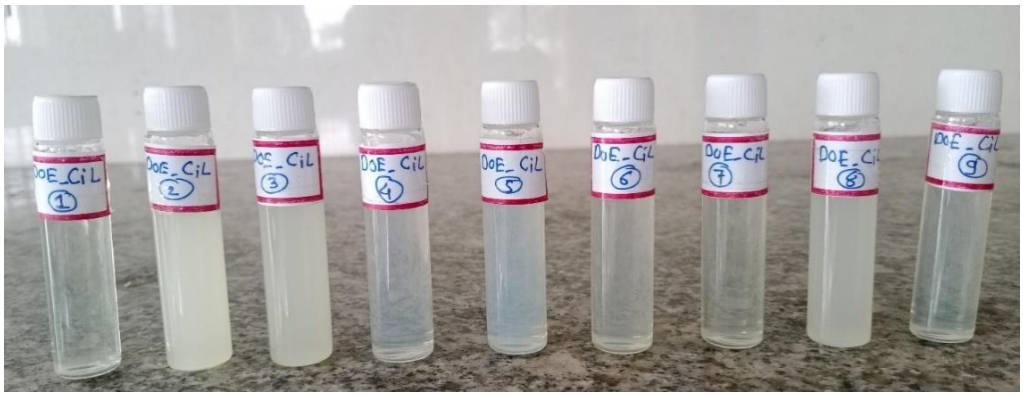

**Fig. 6: Cilnidipine-loaded optimised nanoemulsions**

**Cilnidipine nanoemulsion optimisation results**

The response surface method approximates the correlation function using a complete quadratic equation. The impact of independent variables on particle size (Y1), drug content (Y2), and PDI (Y3) are given in table 4. Polynomial equation coefficients were calculated using experimental data to predict the response variable's values. Regression equations for each response variable, obtained from response surface methodology, are mentioned in

$$Y= \beta0+\beta1A+\beta2B+\beta3AB+\beta4\ A^2+\beta5\ B^2$$

Where Y is the designated response, β0– intercept, β1– β5 are the regression coefficients, A and B are the factors studied,

The relationship between the response model equation and particle size, Drug Content, and PDI is given below:

$$\text{Particle size (Y1)} = +97.60+86.10*A-28.23*B-39.10*AB+73.68*A^2+24.60*B^2 \text{ ---------- (1)}$$

$$\text{Drug Content (Y2)} = +101.00+0.6036*A-0.6250*B-0.1000*AB-0.4644*A^2-1.01*B^2 \text{ ----- (2)}$$

$$\text{For PDI (Y3)} = +0.0.3840-0.1001*A-0.0307*B+0.0055*AB-0.0397A^2-0.0493*B^2 \text{ ------- (3)}$$

The results of the ANOVA are shown in tables 10, 11, and 12. Overall, each model was significant ($p>0.05$). Non-significant terms ($p>0.05$) were removed from equations to simplify models, resulting in the following data.

**Independent variable's impact on the response**

Optimisation by the central composite design and different levels of independent variables were used to synthesise cilnidipine-loaded nanoemulsions, as indicated in fig. 6. Table 9 shows the impact of independent variables on particle size, drug content, and PDI. Table 13 summarises the regression coefficients for the independent variables. The model F-values of 43.88, 5.89, and 19.94 for Particle size, drug content, and PDI, respectively, imply that the model is significant. 3-dimensional surface response plots of the separate process constraints particle size, drug content, and PDI are indicated in fig. 7, 8 and 9, as well as the cumulative effect of independent variables on particle size, drug content and PDI are noted in fig. 10, 11 and 12. The findings indicated that as $S_{mix}$ concentration rises to 35 ml with an ultrasonic irradiation time of 1 min, particle size increases to 382 nm. With an optimum concentration of $S_{mix}$ 30 ml and ultrasonic irradiation time of 3 min, we will get particle size 97.7 nm. For drug content analysis, the concentration of $S_{mix}$ 25 ml with an ultrasonic irradiation time of 5 min drug content was observed at 98.4 %, and $S_{mix}$ 30 and time 3 min will get drug content 101.1 %. As we aimed to minimise the Particle dispersity index, $S_{mix}$ 25 with an ultrasonic irradiation time of 5 min led to generating a PDI of a minimum value of 0.127.

**Table 10: ANOVA study for particle size**

| Source | Sum of squares | df | Mean square | F-value | p-value | |
|---|---|---|---|---|---|---|
| Model | 1.112E+05 | 5 | 22231.44 | 43.88 | <0.0001 | Significant |
| A-$S_{mix}$ | 59309.23 | 1 | 59309.23 | 117.07 | <0.0001 | |
| B-Ultrasonic irradiation time | 6374.01 | 1 | 6374.01 | 12.58 | 0.0094 | |
| AB | 6115.24 | 1 | 6115.24 | 12.07 | 0.0103 | |
| $A^2$ | 37769.01 | 1 | 37769.01 | 74.55 | <0.0001 | |
| $B^2$ | 4209.38 | 1 | 4209.38 | 8.31 | 0.0236 | |
| Residual | 3546.17 | 7 | 506.60 | | | |
| Lack of Fit | 3546.17 | 3 | 1182.06 | | | |
| Pure Error | 0.0000 | 4 | 0.0000 | | | |
| Cor total | 1.147E+05 | 12 | | | | |

**Table 11: ANOVA study for drug content**

| Source | Sum of squares | df | Mean square | F-value | p-value | |
|---|---|---|---|---|---|---|
| Model | 13.92 | 5 | 2.78 | 5.89 | 0.0189 | significant |
| A-$S_{mix}$ | 2.91 | 1 | 2.91 | 6.17 | 0.0420 | |
| B-Ultrasonic irradiation time | 3.13 | 1 | 3.13 | 6.61 | 0.0369 | |
| AB | 0.0400 | 1 | 0.0400 | 0.0847 | 0.7795 | |
| $A^2$ | 1.50 | 1 | 1.50 | 3.17 | 0.1180 | |
| $B^2$ | 7.05 | 1 | 7.05 | 14.93 | 0.0062 | |
| Residual | 3.31 | 7 | 0.4725 | | | |
| Lack of Fit | 3.31 | 3 | 1.10 | | | |
| Pure Error | 0.0000 | 4 | 0.0000 | | | |
| Cor total | 17.22 | 12 | | | | |

**Table 12: ANOVA study for PDI**

| Source | Sum of squares | df | Mean square | F-value | p-value | |
|---|---|---|---|---|---|---|
| Model | 0.1125 | 5 | 0.0225 | 19.94 | 0.0005 | significant |
| A-$S_{mix}$ | 0.0801 | 1 | 0.0801 | 70.99 | <0.0001 | |
| B-Ultrasonic irradiation time | 0.0075 | 1 | 0.0075 | 6.67 | 0.0363 | |
| AB | 0.0001 | 1 | 0.0001 | 0.1072 | 0.7529 | |
| $A^2$ | 0.0110 | 1 | 0.0110 | 9.74 | 0.0168 | |
| $B^2$ | 0.0169 | 1 | 0.0169 | 14.95 | 0.0062 | |
| Residual | 0.0079 | 7 | 0.0011 | | | |
| Lack of Fit | 0.0079 | 3 | 0.0026 | | | |
| Pure Error | 0.0000 | 4 | 0.0000 | | | |
| Cor total | 0.1204 | 12 | | | | |

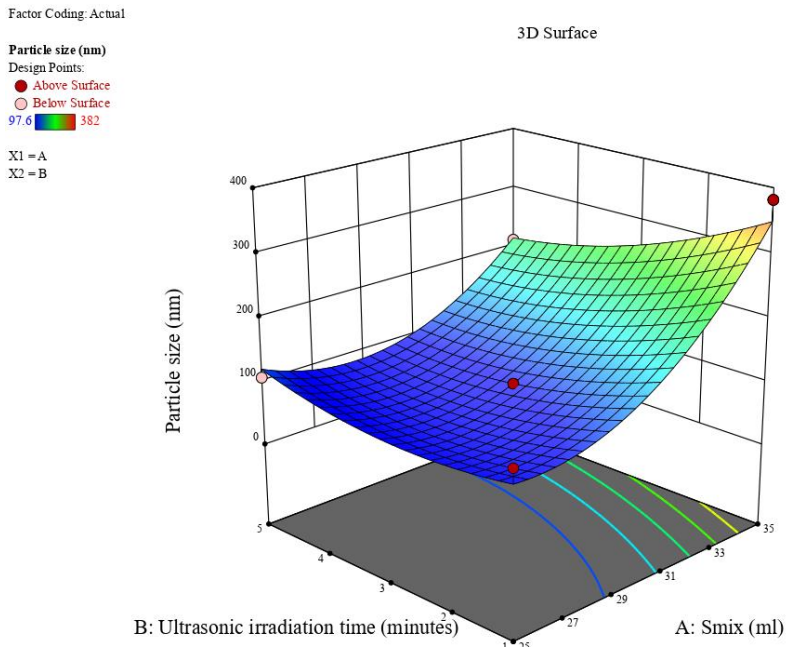


**Fig. 7: 3-D surface response design showing the impact of separate process constraints on particle size**

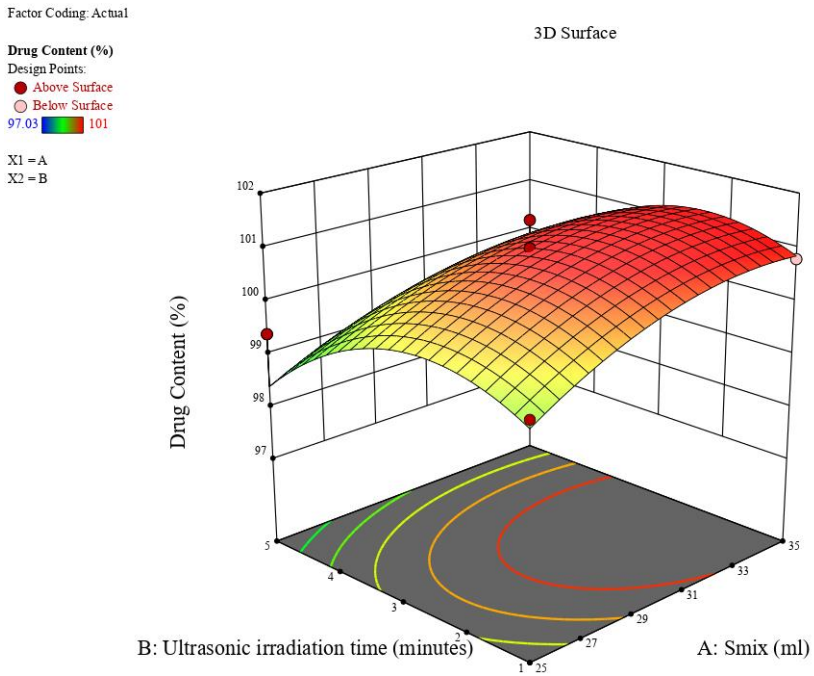


**Fig. 8: 3-D surface response design showing the impact of separate process constraints on drug content**

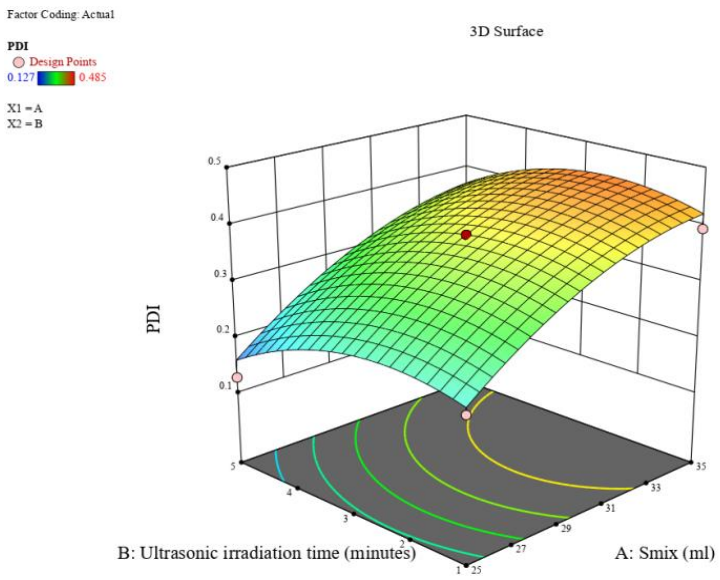


**Fig. 9: 3D surface response design showing the impact of separate process constraints on PDI**

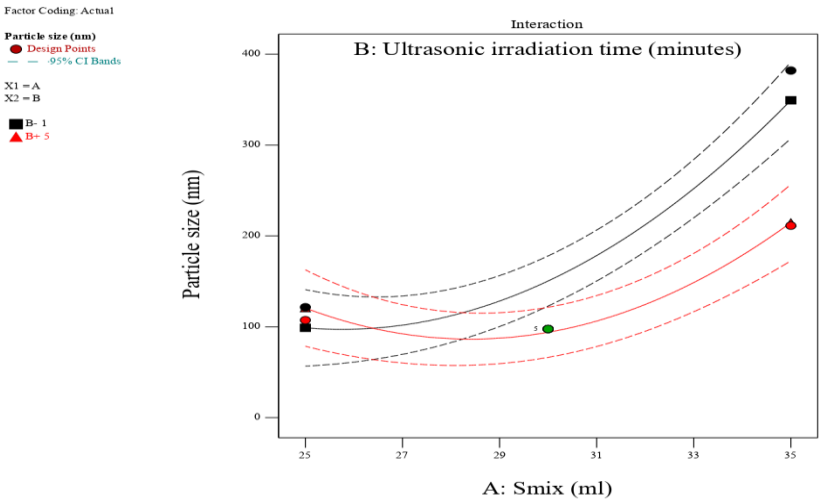


**Fig. 10: Impact of $S_{mix}$ and ultrasonic irradiation time on particle size**

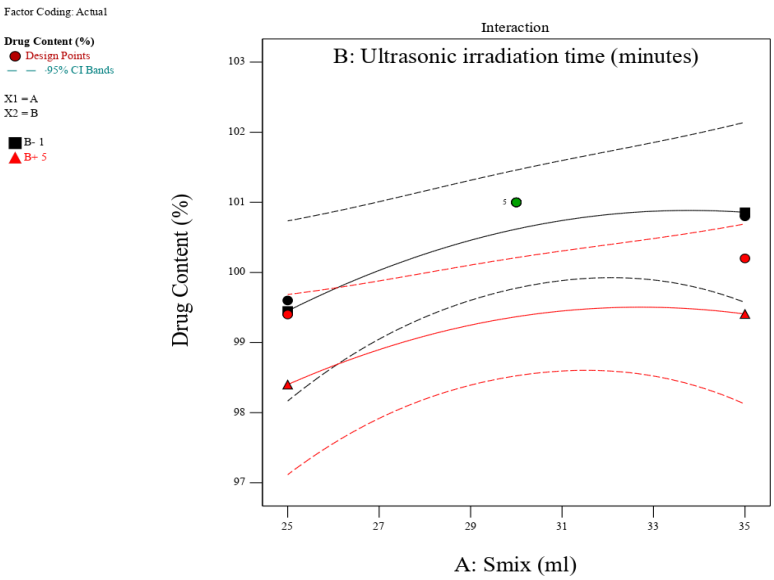


**Fig. 11: Impact of $S_{mix}$ and ultrasonic irradiation time on drug content**

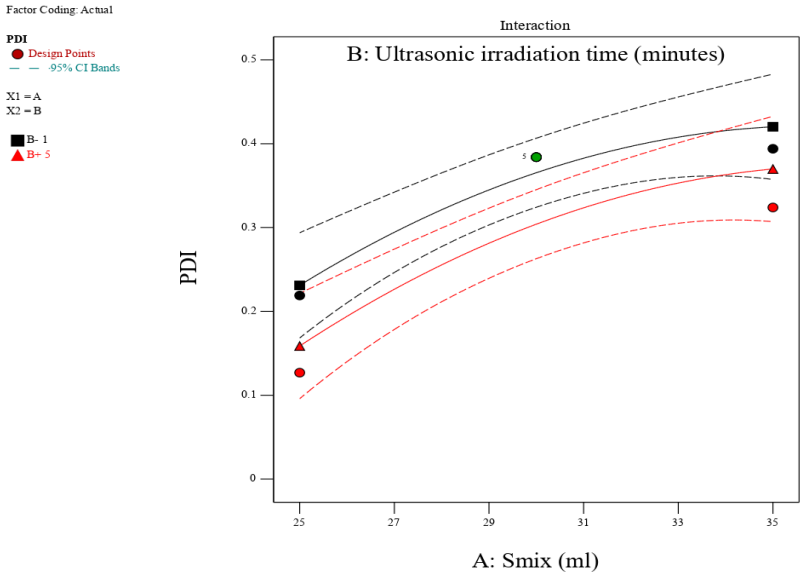


**Fig. 12: Impact of $S_{mix}$ and ultrasonic irradiation time on PDI**

**Table 13: Regression coefficient values for optimised cilnidipine nanoemulsion**

| Regression coefficients | Particle size (nm) | Drug content (%) | PDI |
|---|---|---|---|
| Intercept | 97.60* | 101.00* | 0.3840* |
| A-$S_{mix}$ | 86.10* | 0.6036* | 0.1001* |
| B-Ultrasonic irradiation time | -28.23* | -0.6250* | -0.0307* |
| AB | -39.10* | -0.1000* | 0.0055* |
| $A^2$ | 73.68* | -0.4644* | -0.0397* |
| $B^2$ | 24.60* | -1.01* | -0.0493* |
| $R^2$ | 0.9691 | 0.8079 | 0.9344 |

*Data represented indicates P<0.05

The experimental data could be well represented, according to the results of statistical analysis (ANOVA), by a quadratic polynomial model, with coefficient of determination ($R^2$) values for particle size (Y1), drug content (Y2), and PDI (Y3) being 0.9691, 0.8079, and 0.9344 as shown in table X. Our model is statistically accurate because lack of fit was non-significant ($p<0.05$) with pure error for all variables. It indicates that the model fits the data better if the $R^2$ value is closer to unity. Conversely, response variables are unsuitable for explaining the behavioral variation, according to lower $R^2$ values [52]. The influence of $S_{mix}$ concentration (X1) and ultrasonication irradiation time (X2) on response variables in our study could be suitably described by a quadratic polynomial model, as evidenced by the closeness to 1. Using analysis of variance (ANOVA), the significance level for the quadratic polynomial model's coefficients was established. Larger F-values and smaller P-values suggest that any term significantly impacts the response variable [37].

**Thermodynamic stability studies**

**The cycle of heating-cooling, test for centrifugation, the freeze-thaw cycle**

As per the procedures discussed earlier, we found that NEn_CiL_B1 and C2 formed clear and stable nanoemulsions after a comprehensive thermodynamic stability study [38]. Optimised formulations DOE_CiL_2, 3, and 8 were found unstable after stress testing, while other formulations were observed to have robust stability.

**Characterization of cilnidipine-loaded nanoemulsions**

Cilnidipine-loaded nanoemulsion's Viscosity, pH, and refractive indices were expressed in table 14. The outcomes of the particle size, zeta potential, and Transmission Electron Microscopy of the selected optimised cilnidipine-loaded nanoemulsions are reported in fig. 13 and 14, 15 [35, 38].

**Table 14: Characterisation of optimised cilnidipine-loaded nanoemulsion**

| Code/Design of experiments (DOE) | Viscosity[a] (Pa*s) | pH[a] | Refractive index[a] |
|---|---|---|---|
| DOE _CiL_1 | 0.120±0.00119 | 6.67±0.15 | 1.348±0.04 |
| DOE _CiL_2 | 0.123±0.0061 | 6.16±0.03 | 1.432±0.07 |
| DOE _CiL_3 | 0.137±0.002 | 6.65±0.03 | 1.411±0.04 |
| DOE _CiL_4 | 0.100±0.0021 | 6.16±0.02 | 1.374±0.08 |
| DOE _CiL_5 | 0.0861±0.0011 | 6.38±0.08 | 1.382±0.02 |
| DOE _CiL_6 | 0.121±0.0023 | 7.01±0.13 | 1.401±0.03 |
| DOE _CiL_7 | 0.117±0.00119 | 6.33±0.15 | 1.312±0.06 |
| DOE _CiL_8 | 0.127±0.00144 | 6.79±0.01 | 1.417±0.07 |
| DOE _CiL_9 | 0.0981±0.00283 | 6.28±0.02 | 1.368±0.09 |

[a]Data represented as mean±SEM, n = 3 observations

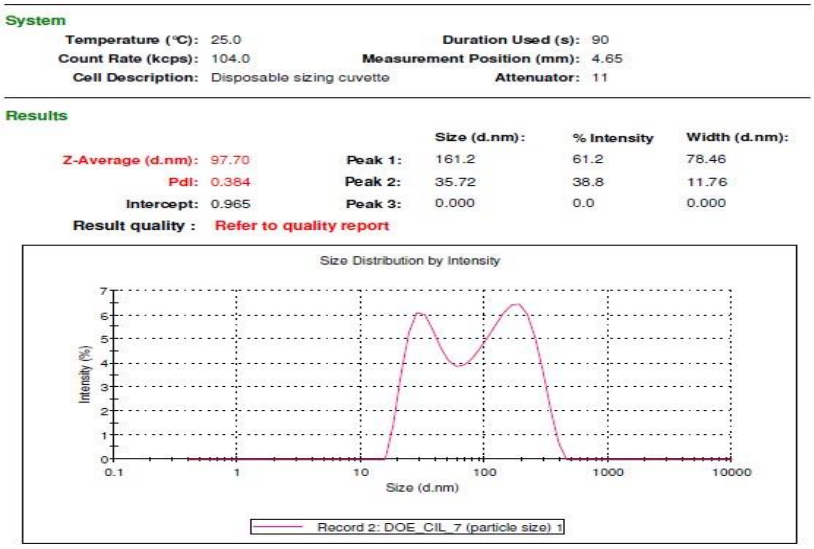


**Fig. 13: Particle size analysis of cilnidipine-loaded nanoemulsion, DOE_CiL_7**

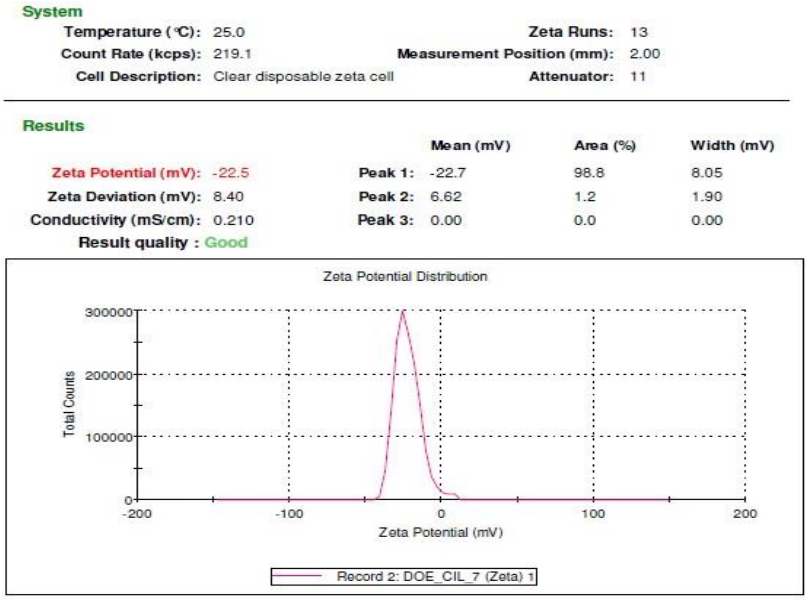


**Fig. 14: Zeta potential of cilnidipine-loaded optimised nanoemulsion, DOE_CiL_7**

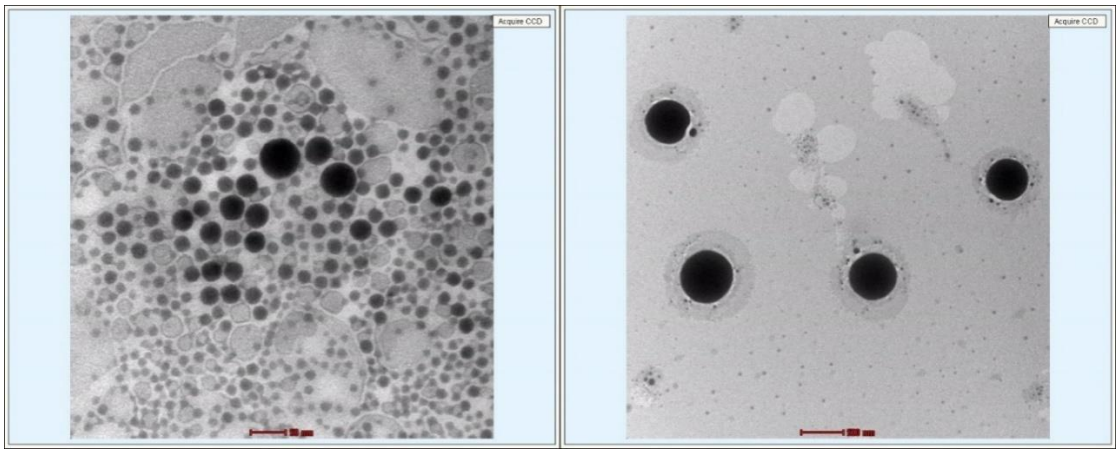

**A** **B**

**Fig. 15: Transmission electron microscopy of cilnidipine-loaded optimised nanoemulsion DOE_CiL7 (A, B), Scale bar is 50 nm; (B) Scale bar is 500 nm**

**_In vitro_ permeation study of optimised cilnidipine-loaded nanoemulsions**

The optimised formulations DOE_CiL_1 to 9 containing 10 mg equivalent cilnidipine were tested for *in vitro* permeation. The cumulative amount permeated from optimised DOE_CiL_1 to 9 nanoemulsions for 0.5 to 24 h is represented in fig.16. The steady-state transdermal flux and permeation coefficient values are displayed in fig. x. The maximum flux in DOE_CiL_7 was 107.7±2.04 µg/cm²/h, and the permeability coefficient was 1.07 cm/h × $10^{-2}$.

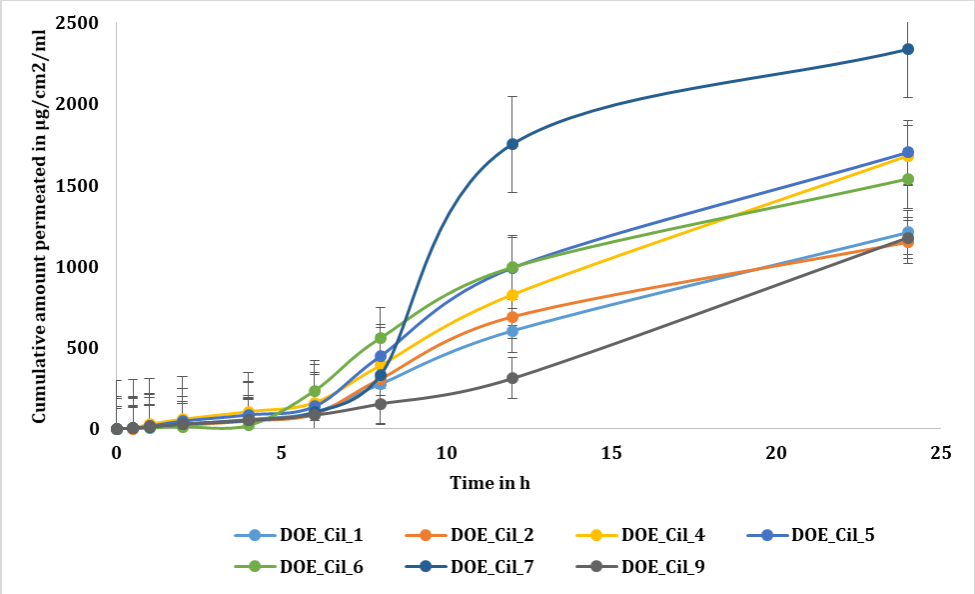


**Fig. 16: Cumulative amount permeated from cilnidipine-loaded optimised nanoemulsions, data represented as mean±SEM, n = 3 observations**

**Table 15: Steady-state flux and permeability coefficients for cilnidipine-loaded optimised nanoemulsions**

| Cilnidipine-loaded optimised NEns | Jss[a] (µg/cm²/h) | Kp[a](cm/h) × $10^{-2}$ |
|---|---|---|
| Calculated flux | 47.5±2.36 | 0.47±0.037 |
| DOE_CiL_1 | 56.65±1.08 | 0.56±0.021 |
| DOE_CiL_2 | 48.59±0.71 | 0.48±0.047 |
| DOE_CiL_3 | 43.97±0.66 | 0.43±0.032 |
| DOE_CiL_4 | 80.65±2.24 | 0.80±0.087 |
| DOE_CiL_5 | 74.45±2.33 | 0.74±0.048 |
| DOE_CiL_6 | 68.84±0.65 | 0.68±0.067 |
| DOE_CiL_7 | 107.7±2.04 | 1.05±0.094 |
| DOE_CiL_8 | 35.71±1.27 | 0.35±0.071 |
| DOE_CiL_9 | 65.14±1.02 | 0.65±0.087 |

[a]Data represented as mean±SD, n = 3 observations

**Formulation and optimisation of cilnidipine-loaded nanoemulsion-gel**

Results showed that some formulations were discarded from simple gel 1 to simple gel 20 (SG1_SG20) due to the low viscosity profiles of simple gels. Only four formulations were decided to contain 1 and 1.5% of Carbopol 940 and four for HPMC $K_4M$. Out of those, Cilnidipine was loaded in Simple Gel 4,10,15,19 (SG 4,10,15,19) to synthesise cilnidipine-loaded formulations re-coded as NEn_CiL_Gel_01 to 04, showing excellent results [40, 41, 44].

**Characterisation of cilnidipine-loaded nanoemulsion-gel**

**Exterior appearance, pH and viscosity**

Results are expressed in table 17. pH of NEn_CiL_Gel_01_04 was noted as 6.21±0.35 to 6.36±0.25 and viscosity values as 3.039±0.0038 to 2.193±0.0037 in Psa [18, 35].

**Spreadability, extrudability**

The table represents the spreadability and extrudability of optimised cilnidipine-loaded nanoemulsion gels (NEn_CiL_Gel_01_04). NEn_CiL_Gel_01_04 shows varied results, with spreadability ranging from 9.52±0.34 to 13.84±0.51 g/cm/s, and excludability is graded [41].

***In vitro* permeation study for cilnidipine-loaded nanoemulsion-based gel**

The developed optimised cilnidipine-loaded nanoemulsion gels (NEn_CiL_Gel_01_04), which contain 1per cent Carbopol 940 (NEn_CiL_04), were selected as the optimised formulation since they have a satisfactory viscosity profile and gelling capacity. The cumulative amount of drug permeated for 0.5 to 24 h from the diffusion membrane was shown in fig. 17, and steady-state transdermal flux and permeability coefficient were reported in table 16. We found a maximum flux from 80.64±1.38 µm/cm²/h for NEn_CiL_Gel_03 and a permeability coefficient of 0.267±0.0045×$10^{-2}$ cm/h. Hence, it is reported that 1% Carbopol 940 gel had 26.703±0.459 maximum flux, and the permeability parameter indicated that the nanoemulsion gel had improved transdermal flux [35, 39].

**Acute dermal toxicity study**

The current study used female Wistar albino rats to investigate the

acute dermal toxicity of cilnidipine-loaded nanoemulsion gel. The results demonstrated that the treatment with cilnidipine-loaded nanoemulsion gel did not cause any evidence of animal death. Additionally, after applying the cilnidipine-loaded nanoemulsion gel, there were no visible signs of erythema (redness) or oedema (swelling) (table 18). The analysis shows no irritation or inflammation on the skin when using the gel formulation. Compared to normal animals, female animals that received topically applied cilnidipine-loaded nanoemulsion gel demonstrated a significant ($P<0.05$) decrease in body weight. Feed and water consumption was not altered significantly (($P<0.05$) by the treatment of cilnidipine-loaded nanoemulsion gel (table 19 and20). Biochemical parameters, including triglycerides, HDL, LDL, total cholesterol, SGOT, and SGPT, were estimated after the experiment. The female animals' biochemical parameters showed no significant ($P<0.05$) changes upon treatment with the cilnidipine-loaded nanoemulsion gel; table 21 reports these findings. Similarly, table 22 indicates no appreciable changes in the animals' absolute and relative organ weights, including the weight of the liver, kidneys, pancreas, thymus, lungs, spleen, and heart, compared to standard control animals. When compared to standard control animals, blood parameters such as haemoglobin, red blood cells (RBCs), white blood cells (WBCs), platelets, and differential white blood cells (WBCs) like monocytes, neutrophils, lymphocytes, eosinophils, and basophils did not significantly change ($P>0.05$) when test compounds were administered (table 23).

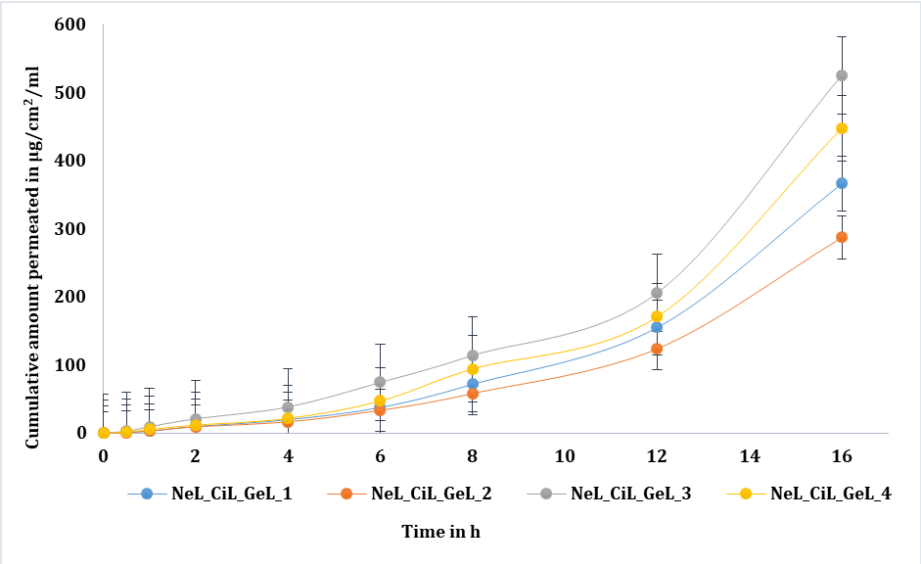


**Fig. 17: Cumulative amount permeated from Cilnidipine-loaded optimised nanoemulsions gels, data represented as mean±SEM, n = 3 observations**

**Table 16: Steady-state flux and permeability coefficients for cilnidipine-loaded optimised nanoemulsion gels**

| Formulation code | Jss[a] (µg/cm²/h) | Kp[a] (cm/h) × $10^{-2}$ |
|---|---|---|
| DOE_CiL_Gel_1 | 52.81±0.938 | 17.486±0. 311 |
| DOE_CiL_Gel_2 | 40.88±1.44 | 13.538±0.478 |
| DOE_CiL_Gel_3 | 80.64±1.38 | 26.703±0.459 |
| DOE_CiL_Gel_4 | 69.24±1.62 | 22.928±0.537 |

[a]Data represented as mean±SD, n = 3 observations

**Table 17: Evaluation of cilnidipine-loaded optimised nanoemulsion gels**

| NEn_CiL_gel formulation code | Clarity | Homogeneity | Consistency | Spreadability[a] (g/cm/s) | Extrudability[a] | pH[a] | Viscosity[a] (Pa*s) |
|---|---|---|---|---|---|---|---|
| NEn_CiL_Gel_1 | ++ | Homogeneous | Better | 9.52±0.34 | +++ | 6.21±0.35 | 4.039±0.0038 |
| NEn_CiL_Gel_2 | ++ | Homogeneous | Better | 5.82±0.62 | ++ | 5.84±0.21 | 6.185±0.0024 |
| NEn_CiL_Gel_3 | +++ | Homogeneous | Excellent | 18.39±0.43 | ++++ | 5.87±0.12 | 8.344±0.0023 |
| NEn_CiL_Gel_4 | +++ | Homogeneous | Excellent | 13.84±0.51 | +++ | 6.36±0.25 | 9.193±0.0037 |

[a]Data represented as mean±SD, n = 3 observations

**Table 18: Effect of cilnidipine-loaded optimised nanoemulsion gel on clinical score of skin and animal mortality**

| Groups | Clinical score[a] | | Animal mortality[a] |
|---|---|---|---|
| | Erythema edema | | |
| Standard control (SC) | 0.0±0.0 | 0.0±0.0 | 0.0±0.0 |
| NEn_CiL_Gel | 0.0±0.0 | 0.0±0.0 | 0.0±0.0 |

[[a]Data represented as mean±SD, n = 5 observations]. *$P<0.05$ significantly different in comparison to Standard control. (Dunnett's multiple comparison t-test is performed after a one-way analysis of variance) (Clinical score: 0: Normal; 1: Mild; 2: Minimal; 3: Moderate; 4 Severe); Abbreviations: SC: Standard Control; NEn_Gel: Nanoemulsion gel

**Table 19: Effect of cilnidipine-loaded optimised nanoemulsion gel onanimal feed consumption**

| Groups | d-1 | d-2 | d-3 | d-4 | d-5 | d-6 | d-7 | d-8 | d-9 | d-10 | d-11 | d-12 | d-13 | d-14 |
|---|---|---|---|---|---|---|---|---|---|---|---|---|---|---|
| | Female rats (g) | | | | | | | | | | | | | |
| Standard control (SC) | 20.96 | 21.51 | 21.85 | 23.64 | 23.66 | 23.21 | 24.13 | 27.93 | 28.13 | 27.95 | 27.89 | 28.97 | 29.53 | 29.07 |
| NEn_Cil_gel | 20.25 | 22.34 | 20.80 | 24.22 | 24.17 | 24.29 | 24.85 | 27.68 | 27.72 | 25.84 | 28.29 | 28.07 | 28.09 | 27.96 |

Abbreviations: SC: Standard control; NEn_CiL_Gel: Cilnidipine-loaded nanoemulsion gel

**Table 20: Effect of cilnidipine-loaded optimised nanoemulsion gel onanimal water consumption**

| Groups | d-1 | d-2 | d-3 | d-4 | d-5 | d-6 | d-7 | d-8 | d-9 | d-10 | d-11 | d-12 | d-13 | d-14 |
|---|---|---|---|---|---|---|---|---|---|---|---|---|---|---|
| | Female rats (ml) | | | | | | | | | | | | | |
| Standard control (SC) | 31.2 | 32.0 | 33.6 | 34.4 | 32.8 | 34.4 | 30.0 | 32.0 | 31.2 | 30.6 | 35.6 | 35.8 | 36.4 | 35.6 |
| NEn_CiL_Gel | 32.0 | 32.4 | 32.0 | 29.4 | 32.6 | 33.6 | 30.6 | 34.4 | 30.4 | 33.4 | 35.2 | 36.2 | 35.2 | 36.0 |

Abbreviations: SC: Standard Control; NEn_CiL_Gel: Cilnidipine-loaded nanoemulsion gel

**Table 21: Effect of cilnidipine-loaded optimised nanoemulsion gel on biochemical parameters**

| Groups | Triglycerides[a] (mg/dl) | HDL[a](mg/dl) | LDL[a](mg/dl) | Cholesterol[a](mg/dl) | SGOT[a](U/l) | SGPT[a](U/l) |
|---|---|---|---|---|---|---|
| | Female rats | | | | | |
| Standard Control (SC) | 98.6±5.2 | 21.7±1.5 | 6.2±1.1 | 54.2±3.4 | 81.1±5.2 | 43.3±3.7 |
| NEn_CiL_Gel | 99.2±6.2 | 22.4±2.5 | 6.1±0.2 | 54.5±3.6 | 81.6±7.4 | 43.6±1.5 |

[[a]Data represented as mean±SD, n = 5 observations]. *P<0.05 significantly different in comparison to Standard control. (Dunnett's multiple comparison t-tests are conducted after one-way ANOVA); Abbreviations: SC: Standard Control; NEn_CiL_Gel: Cilnidipine-loaded Nanoemulsion Gel

**Table 22: Effect of cilnidipine-loaded optimised nanoemulsion gel on organ weight of an animal**

| Groups | Liver (g)[a] | Kidney (g)[a] | Pancreas (mg)[a] | Thymus (mg)[a] | Lung (mg)[a] | Spleen (mg)[a] | Heart (mg)[a] |
|---|---|---|---|---|---|---|---|
| | Female rats (Relative; Per 100 gm of animal) | | | | | | |
| Standard control (SC) | 5.70±0.58 | 1.30±0.19 | 462.64±40.73 | 248.88±22.87 | 724.82±43.70 | 307.37±22.02 | 442.37±42.83 |
| NEn_CiL_Gel | 5.69±0.62 | 1.29±0.10 | 445.52±43.46 | 249.40±12.42 | 701.88±95.51 | 304.96±40.74 | 434.26±71.5 |

[[a]Data represented as mean±SD., n=5 observations]. *P<0.05 significantly different from Standard control. (Dunnett's multiple comparison t-tests are conducted after one-way ANOVA); Abbreviations: SC: Standard Control; NEn_CiL_Gel: Cilnidipine-loaded Nanoemulsion Gel

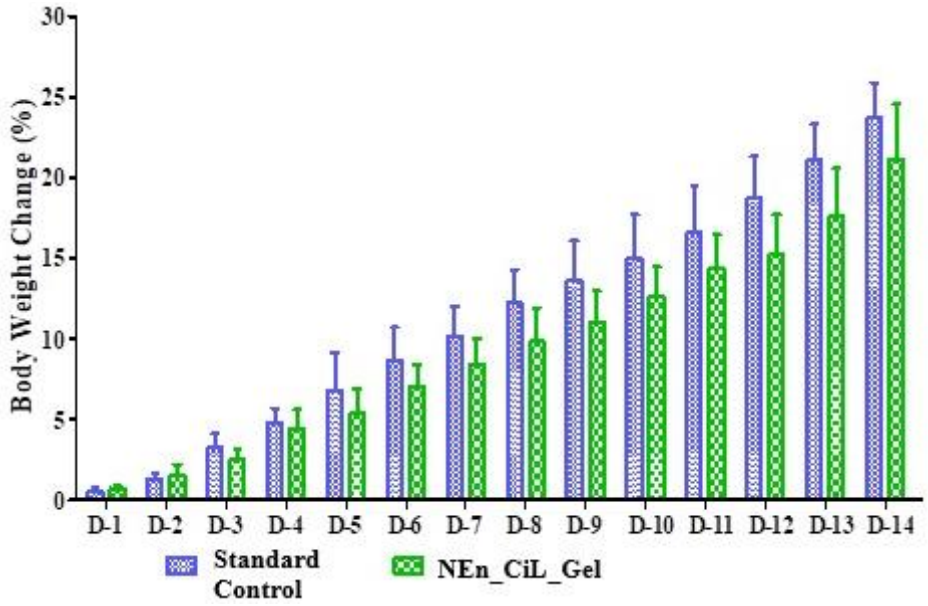


**Fig. 18: Effect of cilnidipine-loaded optimised nanoemulsion gel on animal body weight change (%) A females, [Data represented as mean±SD., n=6 observations]; Two-way analysis of variance is used to analyse the data, and then Bonferroni's multiple comparison t-tests are used.; *P<0.05, **P<0.01, ***P<0.001, significantly different in comparison to Standard control. Abbreviations: SC: Standard Control; NEn_CiL_Gel: Cilnidipine nanoemulsion gel**

**Table 23: Effect of cilnidipine-loaded optimised nanoemulsion gel on haematological parameters**

| Groups | WBCs[a] (10^3/µl) | NEU[a] (%) | LYM[a] (%) | MONO[a] (%) | EOS[a] (%) | BAS[a] (%) | RBCs[a] (10^6/µl) | HGB[a] (g/dl) | MCV[a] (fl) | MCH[a] (pg) | MCHC[a] (g/dl) | PLTs[a] (10^3/µl) |
|---|---|---|---|---|---|---|---|---|---|---|---|---|
| | Female Rats | | | | | | | | | | | |
| Standard control (SC) | 15.2±1.2 | 2.5±0.3 | 6.4±0.8 | 0.6±0.1 | 0.4±0.1 | 0.2±0.1 | 7.3±0.4 | 15.4±0.4 | 51.7±2.7 | 20.8±1.2 | 38.9±1.5 | 909.2±54.2 |
| NEn_CiL_Gel | 15.2±2.0 | 2.5±0.3 | 6.4±1.2 | 0.6±0.1 | 0.4±0.1 | 0.2±0.0 | 7.3±0.2 | 15.4±0.7 | 51.7±2.5 | 20.3±1.1 | 39.8±2.1 | 910.8±67.5 |

[[a]Data represented as mean±SD., n=5 observations]. *P<0.05 significantly different in comparison to Standard control. (Dunnett's multiple comparison t-tests are conducted after ANOVA). Abbreviations: SC: Standard Control; NEn_CiL_Gel: Cilnidipine-loaded Nanoemulsion Gel; WBCs: White blood cells, NEU: Neutrophils, MONO: Monocytes, EOS: Eosinophils, BAS: Basophils, RBCs: Red blood cells, HGB: Hemoglobin, MCV: mean corpuscular volume, MCH: mean corpuscular haemoglobin; MCHC: mean corpuscular haemoglobin concentration, PLTs: Platelets

**Pharmacokinetic study**

The trapezoidal area under the curve (AUC) was computed in the pharmacokinetic (PK)study to evaluate the total drug exposure. Significant differences were observed in evaluating cilnidipine in tablet and cilnidipine-loaded nanoemulsion gel formulations, as shown in table 24. The Cmax for cilnidipine in the tablet was 332.3±14.2 ng/ml, but in the nanoemulsion gel, it increased significantly (P<0.05) to 593.00±24.8 ng/ml. The Tmax for both formulations stayed at 3 h despite this increase. Furthermore, from 1279±34.1 ng/ml, the $AUC_{0-12}$ demonstrated a significant (P<0.05) increase. To 1922.50±162.8 ng/ml·h with the tablet and the nanoemulsion gel. Additionally, the nanoemulsion gel's $AUC_{0-\infty}$ increased from 1395.5±156.7 ng/ml·h to 1962.30±174.9 ng/ml·h. These findings suggest that the nanoemulsion gel formulation offers higher absorption than the cilnidipine tablet.

**Table 24: Effect of cilnidipine-loaded optimised nanoemulsion gel on pharmacokinetic parameters of the drug**

| Formulations | Cmax[a] (ng/ml) | Tmax[a] (h) | $AUC_{0-12}$[a] (ng/ml·h) | $AUC_{0-\infty}$[a](ng/ml·h) |
|---|---|---|---|---|
| Cilnidipine Tablet | 332.3±14.2 | 3.0±0.0 | 1279±34.1 | 1395.5±156.7 |
| NEn_CiL_Gel | 593.00±24.8* | 3.0±0.0 | 1922.50±162.8* | 1962.30±174.9* |

[[a]Data represented as mean±SD., n=3 observations ]; Student's unpaired t-test data analysis; *P<0.05 significantly different compared to cilnidipine Tablet. Abbreviations: Cmax: Peak of maximum concentration; Tmax: Time of maximum concentration; $AUC_{0-12}$: Area under the curve until last observation; $AUC_{0-\infty}$: Area under the curve from time 0 to infinity; NEn_CiL_Gel: Cilnidipine Nanoemulsion Gel

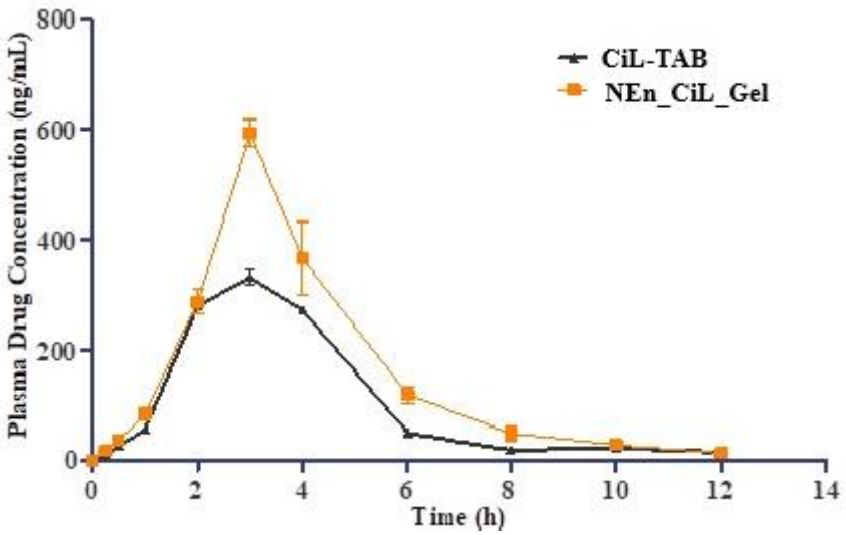


**Fig. 19: Plasma concentration-time profile of cilnidipine-loaded optimised nanoemulsion gel, data represented as mean±SEM, n=3 observations, Abbreviations: CiL-TAB: Cilnidipine tablet; NEn_CiL_Gel: Cilnidipine nanoemulsion gel**

The study demonstrates that cilnidipine-loaded nanoemulsion gel significantly enhances the transdermal delivery of cilnidipine, as evidenced by increased Cmax and AUC. Nanoemulsion delivery through the transdermal route is promising for drugs with rapid first-pass metabolism and very low aqueous solubility. Nanoemulsions minimise interaction with different layers of the skin and could significantly improve drug bioavailability. It also opens up the possibility of terminating therapy with transdermal nanoemulsion, a hopeful prospect. It's a promising development, and studies have already demonstrated that nanoemulsions can boost the bioavailability of poorly soluble medications. Recent studies on enhanced solubility and dissolution rates support the idea that the increased surface area of nanoemulsion droplets facilitates better skin permeation, which accounts for the observed improvements in drug delivery [18, 53, 54]. The cilnidipine-loaded nanoemulsion gels' biocompatibility and stability (data hidden) were verified, and tests on acute dermal toxicity revealed no adverse effects, indicating their safety for use in clinical settings. This discovery emphasises the possible effectiveness of nanoemulsion drug delivery systems. Cilnidipine's dual-action mechanism aligns with recent research highlighting nanoemulsions' benefits in managing hypertension, offering improved drug solubility, sustained drug levels, and enhanced therapeutic outcomes. Challenges such as long-term stability and uniformity of nanoemulsion gels persist and require ongoing optimisation. The smaller droplet sizes of nanoemulsions improve drug absorption by increasing contact area

with the skin, which is crucial for drugs like cilnidipine with limited solubility. The enhanced stability and good release properties of nanoemulsion gels are beneficial for chronic conditions, reducing dosing frequency and improving patient compliance. Reduced systemic side effects due to localised drug delivery are advantageous, especially for drugs with significant systemic effects. This study highlights the need for further research to address scalability and efficacy across diverse patient populations, stressing the urgency and importance of this task. This study contributes to the evidence supporting nanoemulsions and nanoemulsion gels for improved transdermal drug delivery, emphasising the need for further research to address scalability and efficacy across diverse patient populations.

## CONCLUSION

The study assessed cilnidipine's acute dermal toxicity and pharmacokinetics in animal models while evaluating its efficacy in nanoemulsion and cilnidipine-loaded nanoemulsion gel formulations. The study's main conclusions showed that these formulations considerably increased the drug's bioavailability compared to conventional tablets, with high Cmax and AUC values for nanoemulsion gels indicating improved transdermal absorption. Acute dermal toxicity tests demonstrated the safety of these formulations by showing no appreciable adverse effects on organ weights, biochemical parameters, or overall health. The formulations necessary for reliable therapeutic impact also demonstrated stable physical and chemical characteristics, like pH and viscosity. These findings strongly support the safety and stability of nanoemulsion technologies, reassuring the audience about their potential for clinical use and enhancing drug delivery and treatment results.

## ACKNOWLEDGEMENT

Authors are thankful to Gattefossé, India, for providing gift samples of Paceol, Transcutol ® P, Lauroglycol™ FCC, Labrafil M1944, and IMCD India Private Ltd., Bandra (East), Mumbai for gift samples of Kollicream ® OA, Kolliphor ® EL, Kolliphor®RH 40. The authors also thank the principal and staff of R. C. Patel Institute of Pharmaceutical Education and Research, Shirpur, for their help. The authors express deep gratitude towards the Principal, Govt. College of Pharmacy, Chh. Sambhajinagar, for encouragement throughout the work.

## FUNDING

Nil

## AUTHORS CONTRIBUTIONS

Mahesh T. Gaikwad conducted the research, analysed the data, and wrote the manuscript. Dr Rajendra P. Marathe supervised the research project and reviewed and approved the manuscript.

## CONFLICT OF INTERESTS

Declared none

## REFERENCES

1. Shete MM. Cilnidipine: next-generation calcium channel blocker. J Assoc Physicians India. 2016;64(4):95-9. PMID 27734656.
2. Chandra KS, Ramesh G. The fourth generation calcium channel blocker: cilnidipine. Indian Heart J. 2013 Dec;65(6):691-5. doi: 10.1016/j.ihj.2013.11.001, PMID 24407539.
3. Diwan R, Ravi PR, Pathare NS, Aggarwal V. Pharmacodynamic pharmacokinetic and physical characterization of cilnidipine loaded solid lipid nanoparticles for oral delivery optimized using the principles of design of experiments. Colloids Surf B Biointerfaces. 2020 Sep 1;193:111073. doi: 10.1016/j.colsurfb.2020.111073, PMID 32388122.
4. Renjish C, Ittiyavirah SP, Harindran J, Sudhakaran Nair CR. Preparation characterisation evaluation and DFT analysis of cilnidipine-L-phenylalanine cocrystal. Int J Appl Pharm. 2023 Nov 1;15(6):365-72.
5. Cherukkoth R, Ittiyavirah SP, Harindran J, Nair CR. Characterization evaluation and density functional analysis of cilnidipine otinamide cocrystals developed by liquid assisted grinding technique: a sustainable approach for enhanced solubility. Int J Appl Pharm. 2024 Mar 1;16(2):132-8.
6. PN R, ND. Formulation development and characterisation of cilnidipine loaded solid lipid nanoparticles. Asian J Pharm Clin Res. 2018 Sep 1;11(9):120-5. doi: 10.22159/ajpcr.2018.v11i9.24666.
7. Bhalerao A, Chaudhari PP. Formulation of solid lipid nanoparticles of cilnidipine for the treatment of hypertension. J Drug Delivery Ther. 2019 May 15;9(3):212-21. doi: 10.22270/jddt.v9i3.2849.
8. Mankar SD, Tupe A. Solubility enhancement and evaluation of cilnidipine using solid dispersion techniques. Int J Exp Res Rev. 2023;32:347-57. doi: 10.52756/ijerr.2023.v32.030.
9. Karemore MN, Bali NR. Gellan gum-based gastroretentive tablets for bioavailability enhancement of cilnidipine in human volunteers. Int J Biol Macromol. 2021 Mar 31;174:424-39. doi: 10.1016/j.ijbiomac.2021.01.199, PMID 33539955.
10. Anand K, Karmakar S, Mandal P, Shaharyar MA, Bhowmik R, Mondal A. Formulation development optimization and characterization of cilnidipine loaded self microemulsifying drug delivery system. Asian Pac J health Sci; 2021.
11. Khatoon K, Rizwanullah M, Amin S, Mir SR, Akhter S. Cilnidipine loaded transfersomes for transdermal application: formulation optimization *in vitro* and *in vivo* study. J Drug Deliv Sci Technol. 2019 Dec 1;54:101303. doi: 10.1016/j.jddst.2019.101303.
12. Mishra R, Mir SR, Amin S. Polymeric nanoparticles for improved bioavailability of cilnidipine. Int J Pharm Pharm Sci. 2017 Feb 27;9(4):129. doi: 10.22159/ijpps.2017v9i4.15786.
13. Kumar Sharma A, Singh Naruka P, Soni S, Sarangdevot YS, Khandelwal M, Aman S. Development and evaluation cilnidipine fast dissolving tablet by using isapghula husk as natural superdisintegrant. Int J Current Pharm Rev Res. 2019;11(1):1-11.
14. Shaikh F, Patel M, Patel V, Patel A, Shinde G, Shelke S. Formulation and optimization of cilnidipine loaded nanosuspension for the enhancement of solubility dissolution and bioavailability. J Drug Deliv Sci Technol. 2022 Mar;69:103066. doi: 10.1016/j.jddst.2021.103066.
15. Liu Q, Mai Y, GU X, Zhao Y, DI X, MA X. A wet milling method for the preparation of cilnidipine nanosuspension with enhanced dissolution and oral bioavailability. J Drug Deliv Sci Technol. 2020 Feb 1;55:101371. doi: 10.1016/j.jddst.2019.101371.
16. A Alzalzalee R, Kassab HJ. Cilnidipine nanoparticles oral film: preparation and evaluation. JRP. 2024;28(1):191-6. doi: 10.29228/jrp.687.
17. Tandel H, Raval K, Nayani A, Upadhay M. Preparation and evaluation of cilnidipine microemulsion. J Pharm Bioallied Sci. 2012;4 Suppl 1:S114-5. doi: 10.4103/0975-7406.94162, PMID 23066184.
18. Sharma A, Singh AP, Harikumar SL. Development and optimization of nanoemulsion-based gel for enhanced transdermal delivery of nitrendipine using box behnken statistical design. Drug Dev Ind Pharm. 2020;46(2):329-42. doi: 10.1080/03639045.2020.1721527, PMID 31976777.
19. Chapter GA. 21-nanoemulsions. Nanoparticles for biomedical applications. In: Chung EJ, Leon L, Rinaldi C, editors. Micro and Nano Technologies; 2020. p. 371-84. Available from: https://www.sciencedirect.com/science/article/pii/B9780128166628000217elsevier. [Last accessed on 20 Nov 2024].
20. Gheorghe I, Saviuc C, Ciubuca B, Lazar V, Chifiriuc MC. Nanodrug delivery systems for transdermal drug delivery. Grumezescu AM, editor. Chapter 8 nanomater drug delivery ther. William Andrew Publishing; 2019. p. 225-44. Available from: https://www.sciencedirect.com/science/article/pii/B9780128165058000102. [Last accessed on 20 Nov 2024].
21. MC Clements DJ, Jafari SM. General aspects of nanoemulsions and their formulation. Jafari SM, McClements DJ, editors. Chapter 1. Nanoemulsions. In: Academic Press; 2018. p. 3-20. Available from: https://www.sciencedirect.com/science/article/pii/B9780128118382000011. [Last accessed on 20 Nov 2024].
22. Shah MR, Imran M, Ullah S. Nanoemulsions. Chapter 4. Lipid based nanocarriers for drug delivery and diagnosis. Shah MR, Imran M, Ullah S, editors. In: William Andrew Publishing; 2017. p. 111-37. Available from:

https://www.sciencedirect.com/science/article/pii/B9780323527293000044. [Last accessed on 20 Nov 2024].
23. Tirnaksiz F, Akkus S, Celebi N. 9-nanoemulsions as drug delivery systems. In: Monzer F, editor. Colloids in drug delivery. CRC Press, Taylor & Francis Group; 2010. p. 221-44. doi: 10.1201/9781439818268-c9.
24. Aparna C, Srinivas P, Rao Patnaik KS. Enhanced transdermal permeability of telmisartan by a novel nanoemulsion gel. Int J Pharm Pharm Sci. 2015;7(4):335-42.
25. Bali V, Ali M, Ali J. Study of surfactant combinations and development of a novel nanoemulsion for minimising variations in bioavailability of ezetimibe. Colloids Surf B Biointerfaces. 2010 Apr 1;76(2):410-20. doi: 10.1016/j.colsurfb.2009.11.021, PMID 20042320.
26. Borhade V, Pathak S, Sharma S, Patravale V. Clotrimazole nanoemulsion for malaria chemotherapy. Part I: Preformulation studies formulation design and physicochemical evaluation. Int J Pharm. 2012 Jul 15;431(1-2):138-48. doi: 10.1016/j.ijpharm.2011.12.040, PMID 22227344.
27. Chadha R, Bhandari S. Drug excipient compatibility screening role of thermoanalytical and spectroscopic techniques. J Pharm Biomed Anal. 2014 Jan 18;87:82-97. doi: 10.1016/j.jpba.2013.06.016, PMID 23845418.
28. Secilmis Canbay H, Polat M, Doganturk M. Study of stability and drug excipient compatibility of estriol. Bilge Int J Sci Technol Res. 2019 Sep 30;3(2):102-7. doi: 10.30516/bilgesci.582054.
29. Hamza MY, Abd El Aziz ZR, Aly Kassem M, El Nabarawi MA. Loxoprofen nanosponges: formulation characterization and ex vivo study. Int J App Pharm. 2022 Mar 1;14(2):233-41. doi: 10.22159/ijap.2022v14i2.43670.
30. Lakavath SK, Ahad HA. Construction of ternary phase diagram for three component system (oil water surfactant) as a preliminary step before formulating a nanoemulsion. Eur Chem Bull. 2023;12(10):10669-79.
31. Jayapal N, Vamshi Vishnu Y. Formulation and *in vivo* evaluation of self-nanoemulsifying drug delivery system of ramipril in wistar rats. Asian J Pharm Clin Res. 2021;14(7):126-36. doi: 10.22159/ajpcr.2021.v14i7.42003.
32. Modarres Gheisari SM, Gavagsaz Ghoachani R, Malaki M, Safarpour P, Zandi M. Ultrasonic nano emulsification a review. Ultrason Sonochem. 2019 Apr;52:88-105. doi: 10.1016/j.ultsonch.2018.11.005, PMID 30482437.
33. Mohamadi Saani S, Abdolalizadeh J, Zeinali Heris S. Ultrasonic/sonochemical synthesis and evaluation of nanostructured oil in water emulsions for topical delivery of protein drugs. Ultrason Sonochem. 2019 Jul 1;55:86-95. doi: 10.1016/j.ultsonch.2019.03.018, PMID 31084795.
34. Rahma H, Suciati T. Formulation of sodium ascorbyl phosphate (SAP) in to O/W nanoemulsion. Int J App Pharm. 2023 May 1;15(3):242-6. doi: 10.22159/ijap.2023v15i3.46643.
35. Saraswathi TS, Roshini R, Damodharan N, Mothilal M, Janani SK. Development of lipid based vesicles of terbinafine gel for skin delivery by $^{32}$full factorial design. Int J App Pharm. 2024 Jul 7;16(4):231-43. doi: 10.22159/ijap.2024v16i4.50460.
36. Deka T, Das MK, Das S, Das P, Singha LR. Box behnken design approach to develop nano vesicular herbal gel for the management of skin cancer in experimental animal model. Int J App Pharm. 2022 Nov 1;14(6):148-66. doi: 10.22159/ijap.2022v14i6.45867.
37. Jyothi JB. Design of gastroretentive polymeric low density microballoons of mebendazole using response surface. Methodology. 2022;15(7):149-5. doi: 10.22159/ajpcr.2022v15i7.44090.
38. Elmataeeshy ME, Sokar MS, Bahey El Din M, Shaker DS. Enhanced transdermal permeability of terbinafine through novel nanoemulgel formulation; development *in vitro* and *in vivo* characterization. Future Journal of Pharmaceutical Sciences. 2018 Jun;4(1):18-28. doi: 10.1016/j.fjps.2017.07.003.
39. Chauhan SB, Naved T, Parvez N. Formulation and development of transdermal drug delivery system of ethinylestradiol and testosterone: *in vitro* evaluation. Int J App Pharm. 2019 Jan 1;11(1):55-60. doi: 10.22159/ijap.2019v11i1.28564.
40. Nikumbh KV, Sevankar SG, Patil MP. Formulation development *in vitro* and *in vivo* evaluation of microemulsion based gel loaded with ketoprofen. Drug Deliv. 2015 Jun 1;22(4):509-15. doi: 10.3109/10717544.2013.859186, PMID 24266589.
41. Shraddha M, Anuradha S. Formulation and evaluation of emulgel containing coriandrum sativum seeds oil for anti-inflammatory activity. J Drug Delivery Ther. 2019 Jun 15;9(3-s):124-30. doi: 10.22270/jddt.v9i3-s.2808.
42. Ali EM, Mahmood S, Sengupta P, Doolaanea AA, Chatterjee B. Sunflower oil based nanoemulsion loaded into carbopol gel: semisolid state characterization and ex vivo skin permeation. Indian J Pharm Sci. 2023 Mar 21;85(2):388-420. doi: 10.36468/pharmaceutical-sciences.1104.
43. NS, Chandrakala V, Srinivasan S. Review on: effect of oil surfactant and cosurfactant on microemulsion. Int J Curr Pharm Sci. 2022;14(4)23-7. doi: 10.22159/ijcpr.2022v14i4.2011.
44. Gaber DA, Alsubaiyel AM, Alabdulrahim AK, Alharbi HZ, Aldubaikhy RM, Alharbi RS. Nano emulsion based gel for topical delivery of an anti-inflammatory drug: *in vitro* and *in vivo* evaluation. Drug Des Devel Ther. 2023;17:1435-51. doi: 10.2147/DDDT.S407475, PMID 37216175.
45. OECD/OCDE. OECD Guideline for the testing of chemicals. Acute dermal toxicity: fixed dose procedure; 2017. p. 402. Available from: http://www.oecd.org/termsandconditions/. [Last accessed on 20 Nov 2024].
46. Banerjee S, Chattopadhyay P, Ghosh A, Pathak MP, Singh S, Veer V. Acute dermal irritation sensitization and acute toxicity studies of a transdermal patch for prophylaxis against ({+/-}) anatoxin a poisoning. Int J Toxicol. 2013 Jul;32(4):308-13. doi: 10.1177/1091581813489996, PMID 23696561.
47. Nair AB, Jacob S. A simple practice guide for dose conversion between animals and human. J Basic Clin Pharm. 2016;7(2):27-31. doi: 10.4103/0976-0105.177703, PMID 27057123.
48. Pathan IB, Jaware BP, Shelke S, Ambekar W. Curcumin loaded ethosomes for transdermal application: formulation optimization *in vitro* and *in vivo* study. J Drug Deliv Sci Technol. 2018 Apr 1;44:49-57. doi: 10.1016/j.jddst.2017.11.005.
49. Khani S, Keyhanfar F, Amani A. Design and evaluation of oral nanoemulsion drug delivery system of mebudipine. Drug Deliv. 2016 Jul 23;23(6):2035-43. doi: 10.3109/10717544.2015.1088597, PMID 26406153.
50. Smail SS, Ghareeb MM, Omer HK, Al Kinani AA, Alany RG. Studies on surfactants cosurfactants and oils for prospective use in formulation of ketorolac tromethamine ophthalmic nanoemulsions. Pharmaceutics. 2021 Apr 1;13(4):1-13. doi: 10.3390/pharmaceutics13040467, PMID 33808316.
51. Jadhav CM. Investigating application of non aqueous microemulsion for drug delivery: a review. AJBPS. 2014;4(29):1-9. doi: 10.15272/ajbps.v4i29.460.
52. Mehmood T, Ahmed A, Ahmad A, Ahmad MS, Sandhu MA. Optimization of mixed surfactants based β-carotene nanoemulsions using response surface methodology: an ultrasonic homogenization approach. Food Chem. 2018 Jul 1;253:179-84. doi: 10.1016/j.foodchem.2018.01.136, PMID 29502819.
53. Mou D, Chen H, DU D, Mao C, Wan J, XU H. Hydrogel thickened nanoemulsion system for topical delivery of lipophilic drugs. Int J Pharm. 2008 Apr 2;353(1-2):270-6. doi: 10.1016/j.ijpharm.2007.11.051, PMID 18215479.
54. Yusuf NA, Abdassah M, Sopyan I, Mauludin R, Joni IM, Chaerunisaa AY. Improved characteristics of glibenclamide as transethosome vesicular system: physicochemical solubility and *in vitro* permeation study. Int J App Pharm. 2024 Jan 1;16(1):172-85. doi: 10.22159/ijap.2024v16i1.49245.